CHALMERS
UNIVERSITY OF TECHNOLOGY

Dynamic Tailstrike Avoidance Controller for Takeoff and Landing

Design of a scheduled linear quadratic regulator for the prevention of tailstrikes

Master's thesis in System, Control and Mechatronics

Jonathan Ahlström
Gabriel Ingemarsson

DEPARTMENT OF SOME SUBJECT OR TECHNOLOGY
CHALMERS UNIVERSITY OF TECHNOLOGY
Gothenburg, Sweden 2023
www.chalmers.se

Master's thesis 2023

Dynamic Tailstrike Avoidance Controller for Takeoff and Landing

Design of a Scheduled Linear Quadratic Regulator for the Prevention of Tailstrikes

GABRIEL INGEMARSSON
JONATHAN AHLSTRÖM

CHALMERS
UNIVERSITY OF TECHNOLOGY

Department of Electrical Engineering
Division of Systems and Control
Automatic Control group
Chalmers University of Technology
Gothenburg, Sweden 2023

Dynamic Tailstrike Avoidance Controller for Takeoff and Landing
Design of a Scheduled Linear Quadratic Regulator for the Prevention of Tailstrikes
Gabriel Ingemarsson, Jonathan Ahlström

Supervisor: Welsh Pond, Heart Aerospace
Examiner: Balázs Adam Kulcsar, Department of Electrical Engineering

Master's Thesis 2023
Department of electrical Engineering
Division of Systems and Control
Automatic Control group
Chalmers University of Technology
SE-412 96 Gothenburg
Telephone +46 31 772 1000

Cover: A cover of the ES-30

Typeset in LaTeX
Printed by Chalmers Reproservice
Gothenburg, Sweden 2023

Dynamic Tailstrike Avoidance Controller for Takeoff and Landing
Design of a Scheduled Linear Quadratic Regulator for the Prevention of Tailstrikes

Jonathan Ahlström
Gabriel Ingemarsson

Department of Eletrical Engineering
Chalmers University of Technology

Abstract

In this thesis a dynamic controller has been designed for the use of preventing tailstrikes during takeoff and landing. A linear quadratic regulator has been used due to the ease of incorporating reference commands with state control, allowing the controller to be designed for tailstrike prevention without overridering the pilot completely. Different tuning configurations have been explored and evaluated on their response times, tailstrike preventive abilities, wind turbulence mitigation and pilot handling qualities. A single state feedback gain shows promising robustness results and tailstrike preventive abilities but has difficulties fulfilling conflicting handling quality objectives with a single tuning. Gain scheduling allows for a responsive aircraft at low risk for tailstrikes while mitigating excessive pitch attitudes at a high risk for tailstrike. The controller is able to reduce the risk of tailstrikes at takeoff with aggressive tunings, but because of modeling difficulties on ground level a takeoff could not be performed reliably in flight simulator testing. For a full verification of the controller the model needs to be improved for ground level and able to trim for zero velocity. The scheduled gain controller is able to prevent tailstrikes for landing but requires a larger scope of gains at low and high airspeeds to avoid a conservative tuning schedule. Further robustness analysis and flight testing is required to guarantee the safety of the function.

Keywords: tailstrike prevention, control theory, LQR, linear quadratric regulator, electric aircraft

Acknowledgements

Firstly we would like to thank our supervisor and examiner at Chalmers, Proffesor Balázs Adam Kulcár. His guidance, advise and technical expertise in the control theory has been invaluable during the course of this thesis. We could not have done this without you.

We would also like to thank our supervisor at Heart Aerospace, Welsh Pond, for giving us such a warm welcome to Heart Aerospace and the Flight Controls department. We are really thankful for his patience, encouragement and for giving us an insight to the aviation industry.

Lastly we would like to thank Kenzo Sasaki and Ethem Orhan for their technical expertise and patience with our many questions regarding the aircraft model

ChatGPT, or likewise software aid based on artificial intelligence, has not in any shape or form been used during the course of this thesis.

Jonathan Ahlström, Gabriel Ingemarsson, Gothenburg, June 2023

List of Acronyms

Below is the list of acronyms that have been used throughout this thesis listed in alphabetical order:

EAS	Equivalent airspeed
LTI	Linear Time Invariant
LQG	Linear Quadratic Guassian Controller
LQR	Linear Quadratic Regulator
MCAS	Maneuvering Characteristics Augmentation System
MIMO	Multiple Inputs Multiple Outputs
MPC	Model Predictive Control
SISO	Single Input Single Output
TAS	True Airspeed

Nomenclature

Below is the nomenclature of indices, sets, parameters, and variables that have been used throughout this thesis.

Parameters

V_{EF}	Engine failure speed
V_R	Rotation speed
V_1	Maximum speed at which a takeoff can be rejected
V_2	Takeoff safety speed
V_{LOF}	Lift off speed
V_{MC}	Minimal control speed
V_{MCA}	Minimal Control speed air
V_{MCG}	Minimal Control speed ground
V_s	Stall speed
q_∞	Dynamic Pressure
ρ_∞	Air Pressure
C_L	Lift force

Variables

ϕ	Roll attitude, angle around the plane's x-axis
θ	Pitch attitude, angle around the plane's y-axis
ψ	Yaw attitude, angle around the plane's z-axis
p	Angular rate around the plane's x-axis
q	Angular rate around the plane's y-axis
r	Angular rate around the plane's z-axis
u_b	Body velocity in the plane's x-axis

v_b	Body velocity in the plane's y-axis
w_b	Body velocity in the plane's z-axis
x_e	Earth coordinate on the x-axis
y_e	Earth coordinate on the y-axis
z_e	Earth coordinate on the z-axis
γ	Flight path angle
α	Angle of attack, aircraft's pitch relative to the flight path angle
β	Sideslip angle, angle of the aircraft's orientation relative to the heading direction
H	Altitude
x	State vector for the aircraft
u	Inputs of the aircraft
A	State matrix
B	Input matrix
C	Output matrix
D	Feedforward matrix
Q	Cost matrix for the states x
R	Cost matrix for the inputs u
N	Covariance matrix for the
θ_{ref}	Reference pitch attitude
$\dot{\theta}_{ref}$	Reference pitch rate
θ_e	Pitch attitude error
$\dot{\theta}_e$	Pitch rate error

Contents

List of Figures

List of Tables

1

Introduction

According to the European Commission the aviation sector is now one of the fastest-growing sources of greenhouse gas emissions. [12] Even if the sector now only accounts for 2-3% of the total emissions the sector will grow to 12-18% when flight travel becomes more and more accessible to the worldwide population. [30] To mitigate the trend Heart Aerospace has began to develop an electrical aircraft in an effort to steer away from the aerospace industry's dependency on fossil fuels. The aircraft ES-30, a 30 passenger hybrid aircraft, will be designed for short-distance travel.

1.1 Background

A considerable part of aircraft development is about ensuring the safety of the passengers and control of the aircraft. Safety measures includes minimizing failrates, incorporating redundancy, and reducing the human factor. A particular part of aircraft development is defining the flight envelope for different phases of flight, meaning the safe operating limits of the aircraft, and designing flight controls to ensure the aircraft never exceeds the limits. Exceeding the limits may lead to failures and total loss of control of the aircraft.

Failure conditions in the aviation industry are split into four catagories which are ranked according to their severity. *Minor* events *will* occur in the aircrafts lifetime but not reduce the aeroplanes safety significantly, while *major* events *could* occur in the aircrafts liftime and will result in a significant reduction of the safety of the aircraft or an increased workload for the crew. Hazardous events results in large reductions in safety margins or functional capabilities, and a catastrophic event will prevent safe flight and landing.

A major event that can occur is a tailstrike. A tailstrike occurs when the tail of the aircraft hits the ground during take off and landing, an event that would compromise this event could damage the structural integrity of the aircraft. The damages are oftentimes detectable and can be repaired. However, there are cases when the severity of the event will increase. For example if the pitch rate is high during impact, the major event would transform into a hazardous or even a catastophic one. If the damage repairs are done improperly or damages were left undetected a catastophic

may occur a long time after the actual incident.

This Master's thesis will explore and develop a tailstrike avoidance mechanism using dynamic control, in order to minimise the occurrences of tailstrikes.

1.2 Literature Study

In the early beginnings of the aircraft and their wider use during the first world war, the aircraft design was fully able to be flown without automatic control systems (also referred to as open-loop control). The computational complexity of control theory postponed the development to the 1930-1940s, when classic control theory began to see daylight. The second world war spur technological innovation in control theory for tracking purposes, aircraft stabilization, and handling variations in aircraft dynamics, and the so called altitude-speed envelope was expanded. Changes in aircraft mass properties and loss of aerodynamic drag changed the aircraft dynamic modes to the point that the pilot had difficulties with the controllability. This led to a need of analyzing frequency and dynamics more analytically than before. It become evident that the stability of the aircraft varied largely with flight conditions, and needed stability augmentation to work properly in different ranges of altitude and Mach-number. Closed-loop feedback control became neccessary, and in particular, a feedback control that varies with the flight condition. [31]

There are multiple control methods with different levels of implementation difficulty. The classic control method of proportional-integral-derivative control (shortened PID) is the simplest to implement and best fit for individual signals that does not show a complicated coupling with others. Multivariable methods such as the linear quadratic regulator (LQR) or Guassian controller (LQG) is best fit for strongly coupled signals where systems must be treated as whole for a good feedback control. H_∞-control is another approach if robustness through minimized singular values is desirable. [14] Model predictive control (MPC) can be used to take constraints and future values into consideration when computing the control signals, and the method keeps many of the qualities of optimal control methods such as the LQR. [14] [25] Even if the more advanced methods are tempting, using the simplest controller implementation (while still acquring neccessary levels of performance and stability) is a desirable aim.

Real dynamical systems are often nonlinear, and aircraft dynamics is no exception. However due to the slow-varying nature of the nonlinear dynamics, linear control methods can be deployed for aircrafts. Even if the gains of the control system may need to change as the flight conditions change (as touched upon in the above paragraph, this can be referred to as gain scheduling), resorting to linear control methods eases the implementation compared to nonlinear control methods. Other limitations in control design are the impacts of saturation and rate limits, whose consequences can be difficult to analyse in linear control implementations. [14]

On the specific subject of tailstrike prevention, the tailstrike problem is often ad-

dressed with pilot training rather than with technical solutions. However there are cases where a technical solution has been implemented. An example of this is Airbus A320 which has a pitch limiter and a pitch warning system to avoid a tailstrike. [29] Another solution developed by Boeing is the inclusion of a pitch-down command when risking a tailstrike during landing or takeoff. [10] Few other prevention systems were found during a review of the available patents at the European Patent Register. The available patents on the subject of envelope protection functions regarding tailstrikes revolved mostly around awareness or alerting systems [20] [19]. This is consistent with the primary focus being pilot training to prevent tailstrikes.

Considering the literature and patent review above there are none readily available solutions for a tailstrike prevention function using at least multivariable control. However, multivariable control has been to an increasing extent deployed for other purposes in modern aircraft control systems. Multivariable control exhibits the strength of closing the loop for multiple signals and for a whole system at once, avoiding the complexity of constructing one feedback loop at a time (a drawback pertaining to classical control theory). [31] The aircraft industry is therefore not completely foreign to the domain of multivariable control design.

1.3 Objectives and scope

The objective of this thesis is to develop a tailstrike avoidance function for take-off and landing using dynamic control. The specific conditons during these two phases will be investigated and modeled in order to be used in the development of the control algorithm. The prevalence of model uncertainties, wind disturbances, and approximations motivates the use of control methods with robustness properties.

The controller will be evaluated on metrics like stability, controllability, and responsiveness. It will also be compared to how the system preforms with and without the controller.

1.4 Boundaries

This theis is based on the aircraft model given by Heart Aerospace. The model is a nonlinear representation on how the aircraft behaves under different configurations and phases of the flight. The controller that is to be developed will use this model as a plant, and it will only be specifically developed for the landing and the takeoff phase of flight. Only one trim condition each for the two phases will be considered. Also, the same flap and landing gear configuration will be used for the whole operation - the settings of the aircraft will not be changed midflight or -operation.

The controller that is to be developed will be based on a linear representation of the nonlinear dynamics. It will only consider longitudinal states and dynamics, meaning that the yaw and the bank angle are assumed to be zero and the state feedback will not consider any lateral dynamics.

In the case of the controller using information about the aircraft's states and sensor measurements, they will be considered to be precise. No sensor errors will be added, and therefore a state observer will not be developed.

1.5 Ethics

Given previous tailstrikes incidents it can be concluded that tailstrikes are rarely dangerous themselves. However, it can result in undetected damages which require expensive and difficult reparations of the plane. There are cases however where improper reparations after a tailstrike has lead to catastrophic accidents much later, e.g Japan Air Lines Flight 123 and China Airlines Flight 611. [16] [37]

With this in mind it can be concluded that a tailstrike avoidance algorithm can be very positive for the company but also the general public. With a working algorithm material damage, and human suffering can be avoided, along with commercial implications for the airline operator and the Industry. But in order to ensure that tailstrike prevention works as intended, rigorous testing and validation of the dynamic control algorithm is needed.

There are examples where a pitch-control system has lead to fatal accidents. When the Boeing A737 Max was introduced a new feature called Maneuvering Characteristics Augmentation System (MCAS) was included in the the flight control computer. This function can at the risk of stall order the aircraft to pitch down, and the risk of stall is detected by measuring the angle of attack with a sensor. [9]

However, faulty sensor readings led to the MCAS system activating when the aircraft was *not* at risk of stalling. There are two cases when this led to catastrophic accidents. Firstly for the Lion Air Flight 610 on the 29th of October 2018, and secondly for the Ethiopian Airlines flight 302 on the 10th of March 2019. In both these accidents the MCAS system activated and forced the aircrafts into a nose-down attitude which the pilots were unable to recover from. [9] This function was used as a hard limit for stall prevention. In order to avoid a similar problem with the tailstrike avoidance controller it should use soft limits instead of hard limits.

2

Theory

2.1 Modeling and Dynamics

In this section the forces, moments, and other physical properties governing the aircraft behaviour will be disclosed and explained. First the aerodynamical concept of lift and the lift coefficient will be introduced, to then be followed by the equations of motion. These are important to the flight dynamics and thus the application of the controller.

2.1.1 Aircraft Parts and their Aerodynamics

Airfoil and the Lift Equation

The airfoil's ability to produce lift is important to aircraft modeling. Because of the formation of the airfoil the velocities of the airflow will differ between the top and the bottom surfaces. The airfoil will be forced upwards when the top surface pressure decreases relatively to the bottom, creating the lifting forces needed to carry an aircraft. In Figure 2.1 an illustration of a typical airfoil is shown.

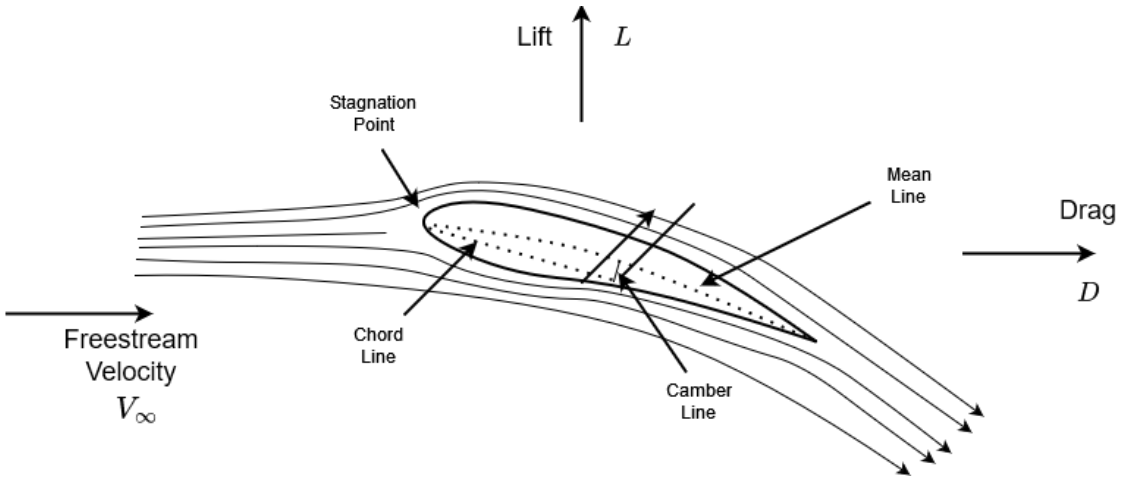

Figure 2.1: Illustration of a typical airfoil. Inspired by Figure 2.2-1 in [31]

The lift equation is central to the aerodynamics of the aircraft. The equation can

used throughout the complete flight envelope, where the lift coefficient becomes the means to adjust the relation after the aerodynamic conditions. [3] The dynamic pressure is

$$q_\infty = \frac{1}{2}\rho_\infty V_\infty \tag{2.1}$$

where ρ_∞ is the air density and V_∞ is the velocity. [2] The lift equation, with the wing area S and lift coefficient C_L, becomes

$$L = q_\infty S C_L = \frac{1}{2}\rho_\infty V_\infty^2 S C_L \tag{2.2}$$

Solving for the lift coefficient

$$C_L = \frac{L}{\frac{1}{2}\rho_\infty V_\infty^2 S} \tag{2.3}$$

The lift coefficient is dependent on the Mach number, the Reynolds number, configuration, and airplane geometry, but has a near linear relation to the angle of attack α up to the maximum α_{max} from which it then falls off. [3] The coefficient is dimensionless [31] and usually determined experimentally. [2]. The angles relations to the reference line is shown in Figure 2.2.

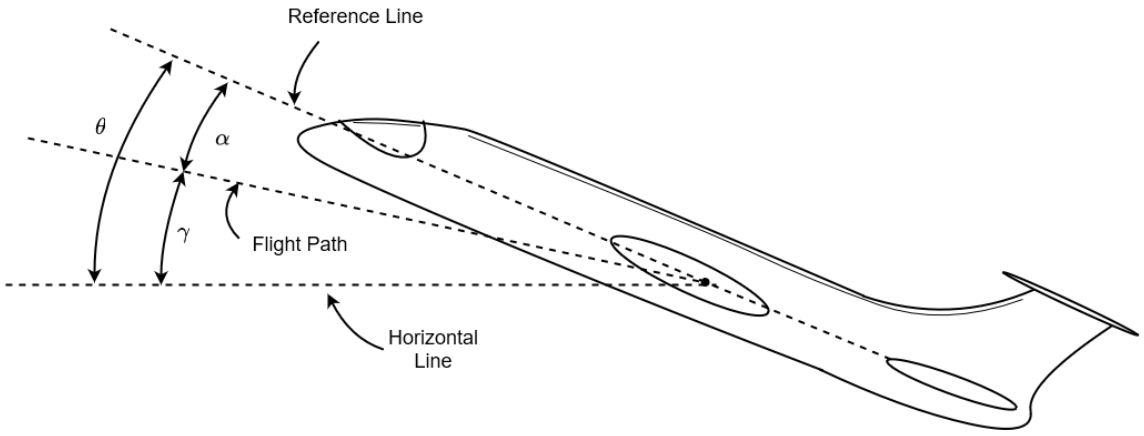

Figure 2.2: Important angles in relation to the aircraft's reference line. Illustration inspired by [5]

The angle of attack α is the difference between the pitch attitude θ and flight path angle γ. The relation is shown in Equation 2.4 and illustrated in Figure 2.3.

$$\theta = \gamma + \alpha \tag{2.4}$$

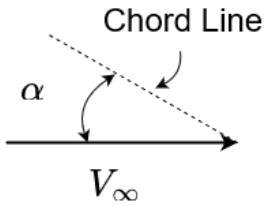

Figure 2.3: Angle of attack relation to the freestream velocity. Illustration based on and inspired by Figure 2.2-1 in [31]

Flight Controls

An aircraft consists of primary and secondary control systems. The primary control surfaces are required to operate the aircraft safely during flights. These consists of ailerons which controls the roll around the longitudinal axis, the elevators that controls the pitch around the lateral axis and finally the rudder which controls the yaw around the vertical axis. The secondary control systems are used to improve the performance characteristics of the aircraft and to assist the pilot. Secondary control systems includes flaps which increase the lift and the induced drag depending on flap position, spoilers which are used to decrese the lift and increase the drag and trim systems which are used to relieve the pilot from keeping a constant pressure on the flight controls. E.g reliving the pilot from holding the sidestick position to keep a constant pitch attitude. [13]

Flaps and Extended Lift

For an airfoil with a particular shape the C_{Lmax} is fixed, and the ability to lift is therefor in practice a function of the velocity V_∞. However there are occasions during flight when another lift-velocity relation is desirable, such as the takeoff and landing phases of flight. [1]

The lowest velocity at which the aircraft can maintain a steady flight is at the stall speed V_{stall}. Considering that an aircraft is confined to a runway for takeoff and landing a lower stall speed will be needed in order to perform a realistic acceleration. By rewriting the lift equation 2.3 the stall speed can be expressed

$$V_{stall} = \sqrt{\frac{L}{\frac{1}{2}\rho_\infty C_{Lmax} S}} \tag{2.5}$$

A lower stall speed is achievable if the lift coefficient C_{Lmax} is increased, and the means to increasing the C_{Lmax} is by extending the wings using flaps. Flaps are adjustable extensions, with multiple possible configurations, located at the back of the wings. When extended and rotated downwards the airfoil becomes more cambered, increasing the pressure difference between the wing surfaces for a specific freestream velocity which in turn enhances the lift of the wing. The C_{Lmax} can be

doubled for the most powerful configuration settings. [1] A conceptual illustration of the airfoil with flaps is shown in Figure 2.4

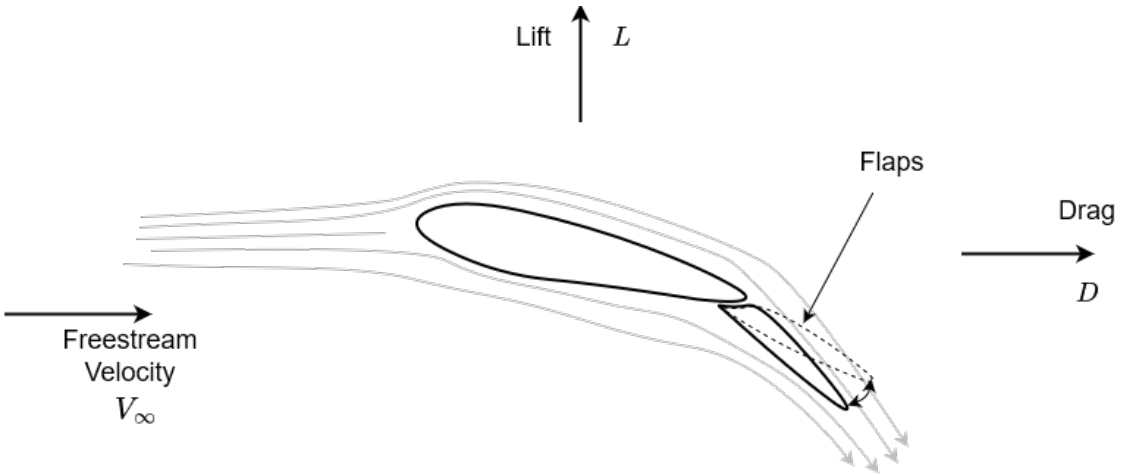

Figure 2.4: Flaps on an airfoil. Illustration based on and inspired by Figure 5.42 in [1] and Figure 2.2-1 in [31]

Increasing the lift is a very apparent desired feature during takeoff, but also during landing. The possibility to slow down (lowering the stall speed) while still maintaining a steady descent is a clear objective during this phase of flight as well. The flaps besides enhancing the lift will at the same time increase the drag, enabling them to be used for braking purposes.

2.1.2 Equations of Motion

An aircraft is subjected to multiple forces and moments that affects the behaviour of the aircraft. The following equations in this chapter have been used to model the aircraft and they use the assumptions of a rigid aircraft travelling around a approximately flat Earth. The model includes the equations of force, moments, kinematics, and navigation. Because of the assumptions and reliance on experimental data the model will by nature be approximative. [31] The model provided by the company is shortly described in the section about Previous work, 2.4.

The source for the force equations stems from the acceleration equation 2.6.

$$(a_i)_B = \dot{\bar{V}}_B + \omega_B \times \bar{V}_B \tag{2.6}$$

The directional velocity and the angular velocity vector for the body is defined as

$$\begin{aligned} V_B &= \begin{bmatrix} U & V & W \end{bmatrix}^T \\ \omega_B &= \begin{bmatrix} P & Q & R \end{bmatrix}^T \end{aligned} \tag{2.7}$$

By developing equation 2.6 the body acceleration components can be expressed in terms of the roll-pitch-yaw rates and angular velocities. Equations 2.8 constitutes

the force equations.

$$\begin{aligned}\dot{U} &= \frac{1}{m}(F_x + RV - QW)\\ \dot{V} &= \frac{1}{m}(F_y + PW - RU)\\ \dot{W} &= \frac{1}{m}(F_z + QU - PV)\end{aligned} \tag{2.8}$$

Equation 2.9 formulates the angular momentum

$$\bar{H} = \bar{r} \times (m\bar{V}) \tag{2.9}$$

and by differentiating the angular momentum

$$\left[\frac{d\bar{H}}{dt}\right]_i = \begin{bmatrix} L & M & N \end{bmatrix}^T \tag{2.10}$$

we gain the moment equations in 2.11. The J-elements are the inertias around their respective axes.

$$\begin{aligned}\dot{P}J_{xx} + QR(J_{zz} - J_{yy}) - (R + PQ)J_{xz} &= L\\ \dot{Q}J_{yy} - PR(J_{zz} - J_{xx}) + (P^2 + R^2)J_{xz} &= M\\ \dot{R}J_{zz} + PQ(J_{yy} - J_{xx}) + (QR - \dot{P})J_{xz} &= N\end{aligned} \tag{2.11}$$

The kinematic equations are

$$\begin{aligned}\dot{\phi} &= P + \tan(Q\ \sin\theta + R\ \cos\phi)\\ \dot{\theta} &= Q\ \cos\phi - R\ \sin\theta\\ \dot{\psi} &= (Q\ \sin\phi + R\ \cos\phi + R\ \sin\phi)/\cos\theta\end{aligned} \tag{2.12}$$

where ϕ, θ, ψ are the Euler angles. The navigation equations are

$$\begin{aligned}\dot{p}_N = U\cos\theta\cos\psi &+ V(-\cos\phi\sin\psi + \sin\phi\sin\theta\cos\psi)\\ &+ W(\sin\phi\sin\psi + \cos\phi\sin\theta\sin\psi)\\ \dot{p}_E = U\cos\theta\cos\psi &+ V(\cos\phi\cos\psi + \sin\phi\sin\theta\cos\psi)\\ &+ W(-\sin\phi\cos\psi + \cos\phi\sin\theta\sin\psi)\\ \dot{p}_D = -U\sin\theta &+ V\sin\phi\cos\theta + W\cos\phi\cos\theta\end{aligned} \tag{2.13}$$

The state vector encompasses all the angles and velocities described in equations , 2.11, 2.12, 2.13 and becomes

$$x = [\ p_N\ \ p_E\ \ p_D\ \ \phi\ \ \theta\ \ \psi\ \ U\ \ V\ \ W\ \ P\ \ Q\ \ R\ ]^T \tag{2.14}$$

2.1.3 Trimming

Trimming is the method of selecting operating points for the aircraft such that the rates of the states are zero or constant. [34] This means if trimmed for a specific condition, such as a certain velocity or a pitch rate, the state will be held without further control input from the pilots. [32] The purpose is to ease the control of the aircraft and reduce the workload for the pilots.

The aircraft can be trimmed for a variety of different phases of flight such as climbing, descent, steady flight and more. Correct trimming is needed for an expected behaviour of the aircraft. An aircraft can be mistrimmed, meaning trimmed for a condition that is not true in the moment.

2.1.4 Longitudinal Dynamics of an Aircraft

The aircraft is characterized by certain behaviours in the longitudinal plane that are called the *short period* and *phugoid* modes. The two motions are two different movement patterns that occur when the aircraft is disturbed from the trim position.

The two modes are described by the characteristic equation in frequency domain, Equation 2.16. The equation stems from first decoupling the equations of motion for the lateral and longitudinal dynamics. The longitudinal dynamics will use the states

$$x = \begin{bmatrix} \theta & Q & U & W \end{bmatrix} \tag{2.15}$$

The transfer function for the longitudinal dynamics will have a denominator of the 4th order which can be shown to be factorised into two 2nd order polynomials, expressing the decoupling between the short period and phugoid modes. [31] The transfer function will not be shown here since it requries additional derivation beforehand, the dampings and the natural frequencies of the modes are of more interest.

$$(s^2 + 2\xi_{SP}\omega_{N_{SP}} + \omega_{N_{PH}}^2)(s^2 + 2\xi_{PH}\omega_{N_{PH}} + \omega_{N_{PH}}^2) = 0 \tag{2.16}$$

These two modes are prevalent for all aircrafts in flight but the dampings ξ and the natural frequency ω_N are a function of the aircraft design and flight conditions. The poles to the characteristic equation should in general be all stable, however the phugoid mode can for some flight conditions be unstable. [38]

In Figure 2.5 a conceptual illustration for the placement of the longitudinal poles is displayed. The precise real- and imaginary values are arbitrarily chosen in the image, but their relative position to each other is based on the pole placements in other works. [28] [22] [27]

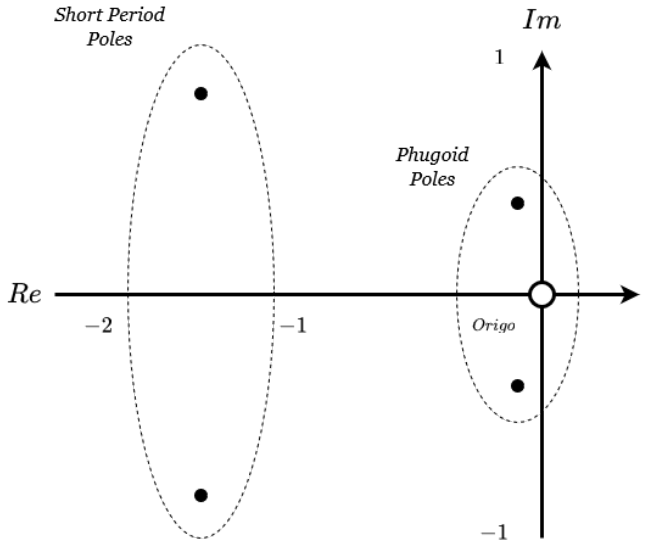

Figure 2.5: Conceptual illustration of the modes' pole placements. The placements are consistent with the results in [28] [22] [27]

Phugoid

The phugoid mode is an oscillatory motion with large variations in pitch attitude and velocity. The aircraft will after a prolonged pitch-up lose airspeed and proceed with a short dive. In the short dive the aircraft will regain its airspeed, regain lift and answer by pitching up. This exchange of kinetic and potential energy will carry on for a longer period. The frequency of the oscillation is lower than that of the short period and has a lower damping ratio as well. [38]

Short Period

The short period mode is the dynamical response of the aircraft to a disturbance to the pitch attitude, for example through a stick command. The pitch attitude θ and angle of attack α will deviate from its trim position for a short while and regain its trim position within a few seconds. It will do so either exponentially or oscillatory, but the response is stable. The motion is characterized by a relatively high damping ratio, relatively high natural frequency, and damped frequency. [38]

2.1.5 Dryden Wind Turbulence Model

The Dryden wind gust turbulence model is a standardized disturbance model for aircraft simulation and testing described in the handbook Military Handbook MIL-HDBK-1797. [33], Military Specification MIL-F-8785C, Military Handbook MIL-HDBK-1797B. [23].

It has been used by the United States Department of Defense and is available as a Simulink^{TM} block in Matlab^{TM} for simulation uses. [23].

The Dryden turbulence model inputs a stochastic process as white noise, and will output the resulting velocities (both regular and angular) from the white noise being filtered through the spectral densities of the velocities. The spectral densities for the velocities are described by equations 2.17-2.19. [33]

$$\Phi_{u_g}(\Omega) = \sigma_u^2 \frac{2L_u}{\pi} \frac{1}{1 + (L_u\Omega)^2} \tag{2.17}$$

$$\Phi_{v_g}(\Omega) = \sigma_v^2 \frac{2L_v}{\pi} \frac{1 + 12(L_v\Omega)^2}{\left[1 + 4(L_v\Omega)^2\right]^2} \tag{2.18}$$

$$\Phi_{w_g}(\Omega) = \sigma_w^2 \frac{2L_w}{\pi} \frac{1 + 12(L_w\Omega)^2}{\left[1 + 4(L_w\Omega)^2\right]^2} \tag{2.19}$$

where L_u, L_v, L_w are turbulence scale lengths and σ_u, σ_v, σ_w are the intensities. Ω is the spatial frequency, defined as $\Omega = \frac{\omega}{V}$, where V is the speed of the aircraft. The angular velocities are instead

$$p_g = \frac{\partial w_g}{\partial y} \tag{2.20}$$

$$q_g = \frac{\partial w_g}{\partial x} \tag{2.21}$$

$$r_g = -\frac{\partial v_g}{\partial x} \tag{2.22}$$

and their spectral densities are expressed as [23]

$$\Phi_p(\Omega) = \sigma_w^2 \frac{1}{2VL_w} \frac{0.8(\frac{2\pi L_w}{4b})^{1/3}}{1 + (\frac{4b\Omega}{\pi})^2} \tag{2.23}$$

$$\Phi_q(\Omega) = \frac{\pm\Omega^2}{1 + (\frac{4b\Omega}{\pi})^2} \Phi_w(\Omega) \tag{2.24}$$

$$\Phi_r(\Omega) = \frac{\pm\Omega^2}{1 + (\frac{3b\Omega}{\pi})^2} \Phi_v(\Omega) \tag{2.25}$$

2.1.6 Ground Effect

The ground effect refers to the specific aerodynamic condition of increased lift when the aircraft is close to the ground. The wings' closeness to the ground dampens the creation of wingtip vortices, thus reducing the induced drag on the aircraft. The reduced drag lowers the thrust needed to gain the appropriate speed and the angle-of-attack required to lift. Because of the ground effect the aircraft may appear to float when approaching the ground during landing. [1]

2.2 Flight Envelope

Flight envelope is a term within aviation which refers to the safe operating limits of the aircraft, and it is within the flight envelope where the structural integrity and manuevrability can be guaranteed. The operating limits can be loosely formulated in terms of airspeed, pressure, altitudes, or angles of attack, and exceeding these limits can lead to a dangerous loss of control or damages to the aircraft. The flight envelope will be different in different phases of flight. An example of exceeding the flight envelope would be to exceed the maximum angle of attack, leading to a loss of lift and the inability to recover the control of the aircraft. For such reasons the aircraft control system needs safety measures that inhibits actions leading to an exit of the flight envelope. [3] [15]

Experiencing a tailstrike can be regarded as exiting the flight envelope when in the development of an envelope protection function. The most prominent risk factors for a tailstrike will therefore be described here. The risks for tailstrike differ for takeoff and for landing, and the risks are therefor divided into two sections. This section will also include a short description of the occurrence of stall.

2.2.1 Tailstrikes at Take-off

In this section the most common reasons for tailstrikes during take-off are explained in short. To ensure that there is a safety margin during the take-off it is important to reach a velocity of $V_{LO} = 1.2V_{stall}$. Where V_{LO} is the lift-of velocity and V_{stall} is the stalling velocity. [1] And the stalling velocity is minimum steady flight speed at which the aircraft is controllable.

The pitch and the pitch rate are in all cases central to the causes, however other errors in computations and trims will increase the aircraft's sensitivity to a tailstrike when applying a pitch command.

Mistrimmed Stabilizer

The horizontal stabilizer is used to balance the aircraft by controlling the rotation around the center of gravity through counteracting the lift of the wings. The resultant moment around the center of gravity will in the trimmed condition equal zero. [21] The stabilizer will affect the pitching ability of the aircraft and mistrimming the stabilizer will greatly enhance the pitch authority at low speeds, resulting in unexpected overrotations of the aircraft. If the pilots trim for an incorrect weight or center-of-gravity the stabilizer will be set in the wrong position. [4]

Rotation at Improper Speed

If the pilot has begun rotation at the improper speed, the aircraft will rotate before having climbed enough into the airspace. This can result in a tailstrike. Usually the speed has been calculated incorrectly or there were other factors that demanded a premature rotation. If the wrong weight is defined the rotation speed V_R will in

turn be computed incorrectly. [4]

Excessive Pitch Rate

The third cause for tailstrike is using an excessive pitch rate. If the pilots are unfamiliar with the sensitivity of the pitch controls this may result in a overrotation and, in turn, a tailstrike. This usually happens when the pilots transition to a new aircraft model. [4]

2.2.2 Tailstrikes at Landing

This section will explain the risks for tailstrike but for landing. An aircraft will be prone to more risks during landing because of the increased freedom of movement in the air. The tailstrikes will also be more severe, since the tail may come down with a larger force onto to the runway. The tail will have to absorb a larger amount of energy during impact and the reparations will cost more in time and resources to perform. [4] The motivations for safeguarding for tailstrikes during landing are therefor particularly strong.

Unstabilized approach

The absolute largest cause to tailstrikes during landing is using a unstabilized approach. If the aircraft is approaching the runway with a velocity or altitude outside the recommended range the pilots will need to resort to more drastic measures to make the runway. Usually the pilots may use an excessive pitch during the flare, causing a tailstrike during touchdown. [4]

Holding Off in the Flare

A pilot conducting an excessively long flare to achieve a smooth landing can cause a tailstrike when the plane drops for touchdown. Also, mistakingly trimming the stabilizers during the flare may cause an unnecessary pitch up of the nose. [4]

2.2.3 Stall

When the angle-of-attack α is increased too far, the airfoil's ability to produce lift falls off. This is what is referred to as stall. The flow will become increasingly detached from the upper surface of the airfoil with higher values of α, eventually detaching already at the front edge. The pressure will change radically, undermining the production of lift and increasing the drag forces instead. [31] The condition of stall is difficult to recover from and must be prevented entirely.

Stall is easier to achieve during descents. The reason for this is that the flight path angle γ is negative, which means that stall can be entered for a lower pitch attitude θ (see Equation 2.4).

2.3 Control Theory

This chapter will introduce the theory behind the control methods used to implement the tailstrike avoidance controller.

2.3.1 State space model

A multiple input multiple output system (MIMO) can be represented using a state space model. The relationship between the inputs and the outputs can be written on the linear time-invariant (LTI) form as

$$\begin{aligned} \dot{x}(t) &= Ax(t) + Bu(t) \\ y(t) &= Cx(t) + Du(t) \end{aligned} \tag{2.26}$$

where x is the state vector of dimension n, u is the input vector of dimension p, y is the output vector of dimesion q and A, B, C, D are matrices with compatible dimensions to x,u and y. [14]

2.3.2 Linear Quadratic Regulator

The linear quadratic regulator (LQR) is a full state feedback controller which aims to minimizes the error from the initial condition or a reference. It is part of the optimal controllers and aims to minimize the quadratic cost function over an infinte horizon.

$$J = \frac{1}{2}\int_0^\infty (x^T Q x + u^T R u + 2x^T N u)dt \tag{2.27}$$

where J is the cost and Q and R are symmetric positive semi-definite weight matrices. Here Q penalizes the states x and R penalizes the control action u. The design parameters are tuned to acquire the preferred controller performance, and the optimal solution is computed as a function of these design parameters. [31] [14] [24]

The feedback control law is designed by solving the following continuous time Riccati quation

$$A^T S + SA - (SB + N)R^{-1}(B^T S + N^T) + Q = 0 \tag{2.28}$$

$$K = R^{-1}(B^T S + N^T) \tag{2.29}$$

where K is the optimal gain matrix and S is the solution to the Riccati quation. [14]

Controllability and Observability

A system is said to be controllable if from a input $u(t)$ and an initial condition $x(0)$ any particular state can be reached within finite time. The controllability criterion can be tested with the controllability matrix S.

$$S(A, B) = [B\ AB\ A^2B\ ...\ A^{n-1}B] \tag{2.30}$$

Here n is the order of the system. The system is controllable if the matrix S does not lose rank.

A system is said to be observable if it does not contain any unobservable states. An observable state is a state which can be estimated using the systems outputs. Similarly to controllability the observability criterion can be tested using the observability matrix O.

$$O(A, C) = \begin{bmatrix} C \\ CA \\ ... \\ CA^{n-1} \end{bmatrix} \tag{2.31}$$

The system is said to be observable if O does not lose rank. If a state space representation of the system is both controllable and observable it is the minimal realisation of the system. Meaning that there is no state representation with lower dimension which displays the same input-ouput relation. [14]

Robustness Properties

Robustness is the property of a controller's ability to handle model uncertainties. [14] Model uncertainties can be errors or unknowns in the model of a system, and a nonlinear model can itself be represented as a linear model with the addition of an uncertainty to one or more parameters.

If a controller is to be considered robust the closed-loop system should be able to remain stable for a degree of model uncertainty. [14]

A controller like the linear quadratic regulator has been shown to have good robustness properties if there are no errors in the measurements of the state. [14] Theoretically it should be able to handle a degree of nonlinearity.

However, adding an observer in the case of non-accurate measurements will also negate any robustness properties of the LQR. Incorporating a Kalman filter to form the linear quadratic Gaussian controller (LQG) will in fact give no robustness guarantees whatsoever. [11]

2.3.3 Matrix Norms and Singular Values

When analyzing MIMO state-space models and transfer functions it is interesting to evaluate the size of the system. The singular values σ of a system represent the principal gains of the system and are defined as the square-root of the system's G eigenvalues [36]

$$\sigma_i [G] \triangleq +\sqrt{\lambda [G^H G]} \tag{2.32}$$

A system of the size (n, n) has n singular values. The singular values σ_{max} and σ_{min} represent the maximal and minimal gains of the system. The infinity norm $\|G\|_\infty$ is equal to the σ_{max} over all frequencies [36]

$$\|G\|_\infty \triangleq \max_i \sum_{j=1}^{n} |G_{ij}| \tag{2.33}$$

2.4 Previous Work

This section will briefly describe the nonlinear aircraft model of the ES30. This is not our own work, but is neccessary background to understand the thesis ahead. The thesis will use this model for developing a controller.

2.4.1 Aircraft State Model

This section describes the inputs, states and outputs of the preexisting nonlinear model of the aircraft.

Inputs

Table 2.1 displays the inputs that are used to control the aircraft. The pilot commands used to adjust the attitude of the aircraft have a input range of -1 to 1, corresponding to a negative or positive deflection of the control surfaces. The pilot uses the stick for a change in pitch and roll attitudes, and the pedals for the yaw.

At zero airflow the maximum command will correspond to maximum deflection, but when the control surfaces are subjugated to enough pressure the control surfaces cannot be fully extended even for full pilot input. However, full extensions are not needed for a significant aircraft response.

The aircraft consists of four separate motors, two on each wing. They are denoted after their side placement (left or right) and placement on the wing (inner or outer). The thrust input 0 to 1 corresponds to a percentage of thrust, from 0% to 100%. The thrust of the four motors is always uniform.

The flap command has four settings which corresponds to the angle of deflection on the flaps. Input settings 0, 1, 2, 3 correspond to the flap deflections of 0°, 15°, 25°,

and 35°. More extension grants a higher lift coefficient and thus lower possible flight speeds.

The landing gear has a binary setting of 1 or 0, either they are extended or not.

Input	min	max	Actuator
aileronCmd*	-1	1	Ailerons
elevCmd*	-1	1	Elevators
rudderCmd*	-1	1	Rudder
flapCmd	0	3	Flaps
thrustOLCmd	0	1	Motor
thrustILCmd	0	1	Motor
thrustIRCmd	0	1	Motor
thrustORCmd	0	1	Motor
landinggearCmd	0	1	Landing Gear

Table 2.1: Inputs for controlling the aircraft.

*These commands have renamed from the model in the report. They were previously named rollCmd, pitchCmd, and yawCmd. This is to differentiate the *pilot's command*, which may be referred to as a pitch command, from the signal that controls the actuator.

States

The nonlinear aircraft model is based on equations of motions decsribed in 2.1.2, equalling a number of 12 states. The states describe the dynamics of the aircraft, but also the dynamics of the control surfaces and their actuators. By including the control surfaces (two ailerons, rudder, and elevator) the amount of states increase to 16.

φ	rad
ψ	rad
θ	rad
p	rad/s
q	rad/s
r	rad/s
u_b	m/s
v_b	m/s
w_b	m/s
x_e	m
y_e	m
z_e	m

Table 2.2: States of the aircraft

Outputs

The outputs of aircraft are dependent on the sensor readings and presented in Table 2.3. Besides the aircraft's attitude and velocity the outputs also include the angle of attack α, the bank angle β, and the flight path angle γ.

α	deg
β	deg
γ	deg
n_z	-
H	m
φ	deg
θ	deg
ψ	deg
p	deg/s
q	deg/s
r	deg/s
V_x	m/s
V_y	m/s
V_z	m/s

Table 2.3: Outputs of the aircraft

3

Methods

3.1 Modeling and Aerodynamics

In this section the approach of modeling the airplane dynamics will be explained. The preexisting nonlinear model will be used as a starting point, but to develop a model-based controller additional steps are to be taken.

3.1.1 Trimming

The trimming of the aircraft is done in Matlab using the built in function *findop()*, which is used to find steady state operating points taking some specifications into consideration. There are a number of constraints set to the input, states and outputs.

There are several optimization options that can be used for the trimming. The one that is used for this model is "graddescent-proj" which makes certain that the derivatives of the states is equal to zero. The outputs are ensured to be equaled to the their predefined values. The optimization also minimizes the error between the states and inputs and their predefined operating point. It also specifies whether the constraints are hard of soft. [26]

The aircraft behaviour is heavily defined by the trim. The aircraft will be trimmed separately and specifically for the two flight operations landing and takeoff, since the flight conditions differ in both cases.

Trimming for landing

The aircraft will be trimmed for the conditions just before descent onto the runway. This includes a low altitude in the 100 meters range, a thrust adapted for a steady descent of $\gamma = -1°$, and a slightly positive pitch. The trim is free to set the thrust levels, and the attitude is trimmed for using the stabilizers on the aircraft. The second flap setting, an extension by 25°, will be used.

State	Value	Dimension
ϕ	0	rad
θ	0.019969	rad
ψ	0	rad
p	0	rad/s
q	0	rad/s
r	0	rad/s
u_b	55.2369	m/s
v_b	0	m/s
w_b	2.0681	m/s
x_e	0	m
y_e	0	m
z_e	-100	m

Input	Value
aileronCmd*	0
elevCmd*	0
rudderCmd*	0
flapCmd	2
thrustOLCmd	0.18
thrustILCmd	0.18
thrustIRCmd	0.18
thrustORCmd	0.18
landinggearCmd	1

Table 3.1: Operating point selected by the trim for the landing

Output	Value	Dimension
α	2.1442	deg
β	0	deg
γ	0	deg
n_z	0.9998	-
H	100	m
φ	0	deg
θ	1.1442	deg
ψ	0	deg
p	0	rad/s
q	0	rad/s
r	0	rad/s
Flap	25	degrees
Elevators	0	degrees
Stabilizer	-2.2319	degrees

Table 3.2: Resulting steady state output for landing

Trimming for takeoff

Trimming for takeoff is more difficult than trimming for landing - the aircraft cannot be trimmed for standing on the ground. The approach is instead to trim for a short distance over ground and let the aircraft drop. When the aircraft has stabilized it is ready to use for takeoff.

To let the aircraft fall to the ground the initial thrust is disconnected, meaning that the aircraft will not have enough thrust to keep a level flight. This also leeds to a drop in the velocity of the aircraft. For this specific trim the speed at which the rotation should begin is $V_r = 93.6$ knots which is around 48 m/s.

State	Value	Dimension
ϕ	0	rad
θ	0.038768	rad
ψ	0	rad
p	0	rad/s
q	0	rad/s
r	0	rad/s
u_b	54.329	m/s
v_b	0	m/s
w_b	2.1073	m/s
x_e	0	m
y_e	0	m
z_e	-10	m

Input	Value
aileronCmd*	0
elevCmd*	0
rudderCmd*	0
flapCmd	2
thrustOLCmd	0.23422
thrustILCmd	0.23422
thrustIRCmd	0.23422
thrustORCmd	0.23422
landinggearCmd	1

Table 3.3: Operating point selected by the trim for the takeoff

Output	Value	Dimension
α	2.2213	deg
β	0	deg
γ	0	deg
n_z	0.99534	-
H	5	m
φ	0	deg
θ	2.2213	deg
ψ	0	deg
p	0	rad/s
q	0	rad/s
r	0	rad/s
Flap	25	degrees
Elevators	0	degrees
Stabilizer	-2.3019	degrees

Table 3.4: Resulting steady state output for takeoff

3.1.2 Longitudinal and Lateral Control

Since the bank and yaw angles are assumed to be zero and not subjected to change, the longitudinal and lateral dynamics will be decoupled and the linearized state-space model can therefore be separated into a longitudinal form and a lateral form. Decoupling the dynamics simplifies the control design while still being accurate, presuming that the conditions continue to apply. By only taking the pitch and thrust command into consideration as inputs and the dynamics in $x-$ and $z-$axes as states the system can be reduced to its longitudinal dynamics.

3.1.3 Linearization

The linearization of the model is performed at the operating points calculated in the trimming. The linearized form can at these specific operating points approximate the behaviour of the nonlinear model and ease the implementation of a controller. The purpose of linearizing is to eventually be able to use controllers based on linear control laws. The Matlab command *linearize()* is used to find the linear approximation and express it on state-space form.

In this subsection the linearization of the nonlinear model using *linearize()* is described. The operating point is found by the trimming algorithm. The aircraft has been trimmed for the landing operation with conditions just before descent. The operating points are described in 3.1

The linearization is besides based on the trim also based on the selected inputs and outputs. The selection of inputs and outputs will define which dynamics are to be considered by the function, and so the inputs and outputs must be carefully chosen such that the appropriate states are included in the linearized state-space model. The inputs and outputs are chosen as the following

Inputs	**Outputs**
aileronCmd	TAS
elevCmd	n_z
rudderCmd	γ [rad]
flapCmd	α [rad]
thrustOLCmd	β [rad]
thrustILCmd	ϕ [rad]
thrustIRCmd	θ [rad]
thrustORCmd	ψ [rad]
-	V_x [m/s]
-	p [rad/s]
-	q [rad/s]
-	r [rad/s]

Table 3.5: The selected inputs and outputs

The linearization function then outputs a model on state-space form, formulated as

$$\dot{x} = Ax + Bu \tag{3.1}$$
$$y = Cx + Du \tag{3.2}$$

with the states, inputs, and outputs of Tables 3.6 and 3.7.

States	Dimensions
φ	rad
ψ	rad
θ	rad
p	rad/s
q	rad/s
r	rad/s
u_b	m/s
v_b	m/s
w_b	m/s
z_e	m

Table 3.6: States of the linearized state-space model

Inputs	Dimensions
pitchCmd	-
thrustOLCmd	-
thrustILCmd	-
thrustIRCmd	-
thrustORCmd	-
rollCmd	-
yawCmd	-
flapCmd	-

Outputs	Dimensions
α	deg
β	deg
γ	deg
n_z	-
H	m
TAS	m/s
φ	rad
θ	rad
ψ	rad
p	rad/s
q	rad/s
r	rad/s
V_x	m/s

Table 3.7: Inputs and outputs of the linearized state-space model

Reduction to Longitudinal States

As described in section 3.1.2 the bank angle β and yaw angle ψ are assumed to be zero, and therefore the system can be reduced to its longitudinal states, inputs, and outputs. The angles ϕ, ψ and their angular rates are omitted as states, and so is the body velocity v_b in the y-direction. The inputs are reduced to only include the pitch and thrust commands. Outputs dependent on the omitted states are also eliminated. Tables 3.8 and 3.9 describe the state, inputs, and outputs used in the longitudinal state-space model.

States	Dimensions
θ	rad
q	rad/s
u_b	m/s
v_b	m/s
z_e	m

Table 3.8: States of the longitudinal state-space model

Inputs	Dimensions
pitchCmd	-
thrustOLCmd	-
thrustILCmd	-
thrustIRCmd	-
thrustORCmd	-

Outputs	Dimensions
α	deg
β	deg
γ	deg
n_z	-
H	m
TAS	m/s
θ	rad
q	rad/s
V_x	m/s

Table 3.9: Inputs and outputs of the longitudinal state-space model

3.1.4 Impulse Response Comparisons

To assess the linearization the system is excited by a input perturbation on the pitch command. If the linearization is accurate the linear system and the nonlinear systems should output near the same responses for very small input perturbations. This is necessary in order to ensure correct controller output. The responses are plotted in Figures 3.1 and 3.2. The impulse responses of the linear system resembles the nonlinear systems quite accurately, although it does grow inaccurate over time. There is a small time delay between the responses, where the linear model is faster.

Both systems also display the modes of the longitudinal dynamics in practice, where the aircraft slowly returns to its trimmed position in a oscillatory manner after a pitch-up command. Because the pitch-up command was short (1 second) it should resemble the short period dynamics but the oscillations remain longer than expected. The system responses are all stable.

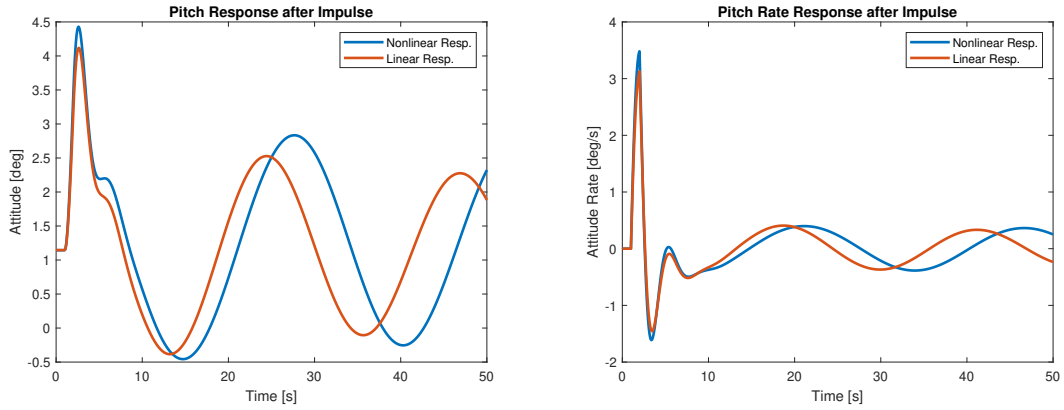

Figure 3.1: The response of the pitch and pitch rate after an input perturbation

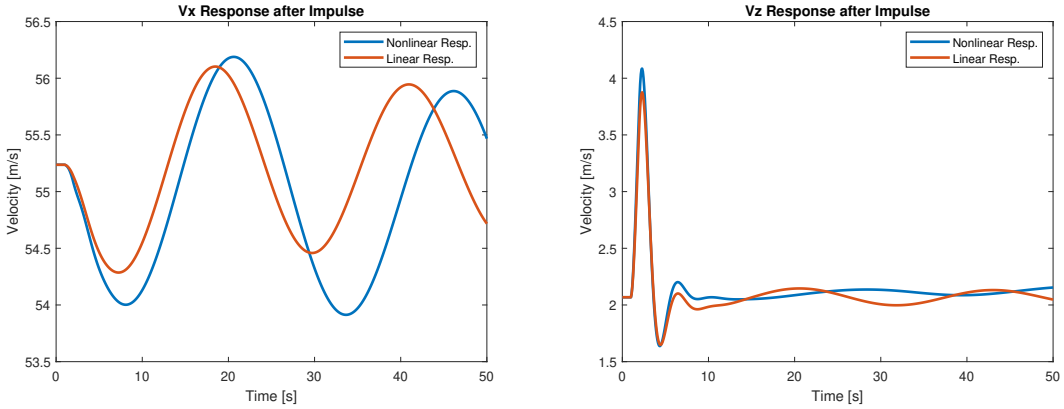

Figure 3.2: The response of the body velocity in x- and z-direction after an input perturbation

3.1.5 Stability Analysis

The stability of the system can be given by observing the eigenvalues. In Figure 3.3 the poles for the short period, the phugoid dynamics, and the height are plotted on a pole-zero map using the landing trim, with the real values on the x-axis and the imaginary values on the y-axis. The poles are all clearly stable for the short period and the phugoid, which shows that the aircraft over time should revert to its trimmed position. However, it will do so in an oscillatory manner.

The fifth eigenvalue correspond to the displacement in the z-axis, z_e.

The same plot for the takeoff trim will be omitted, since the initial conditions for the velocity and thrust needs to be altered in simulation. The poles of the linearized system will then not be completely accurate.

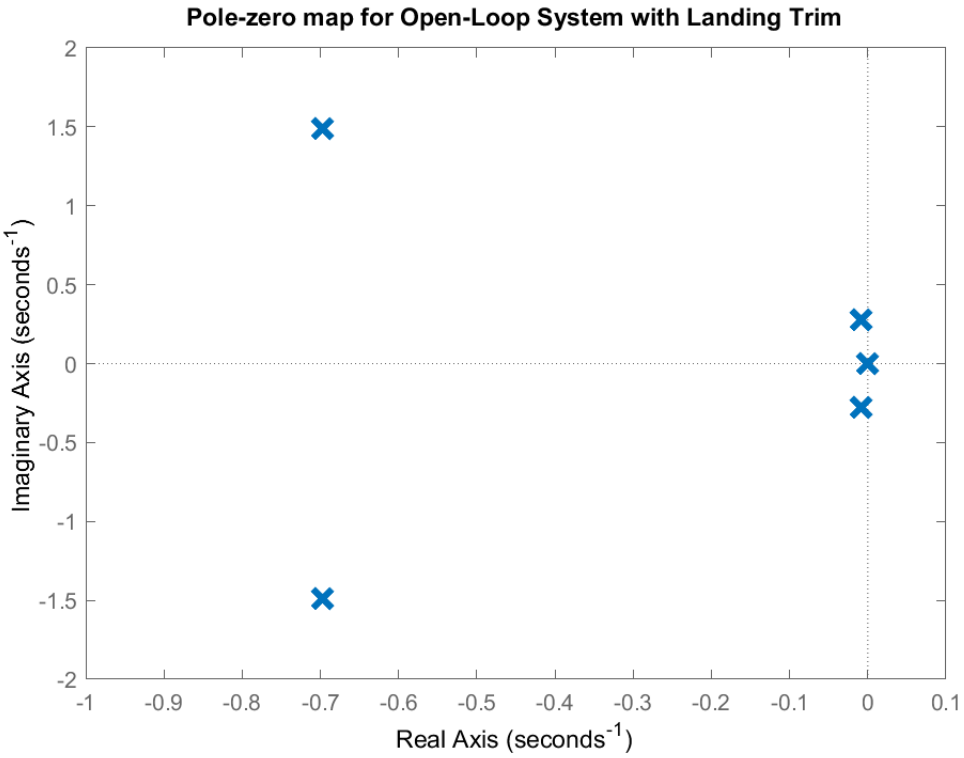

Figure 3.3: Short period and phugoid mode poles for the linearized system around the landing trim

In Figure 3.4 the singular values are plotted for the longitudinal states using the landing trim. The singular values are plotted as a function of frequency. Two of the singular values are closed to zero and are excluded from the plot. The system has a resonant peak at $\omega = 0.284$ rad/seconds with a magnitude of

$$\|G\|_\infty \approx 2900 \tag{3.3}$$

The system has a maximum gain of

$$\max\|G\|_\infty \approx 1.2 \cdot 10^4 \tag{3.4}$$

which is achieved at low frequencies of $\omega = 10^{-4}$. The height output H_m is a dominant contributor to the infinity norm. If omitted, the infinity norm is reduced to

$$\|G\|_\infty \approx 800 \tag{3.5}$$

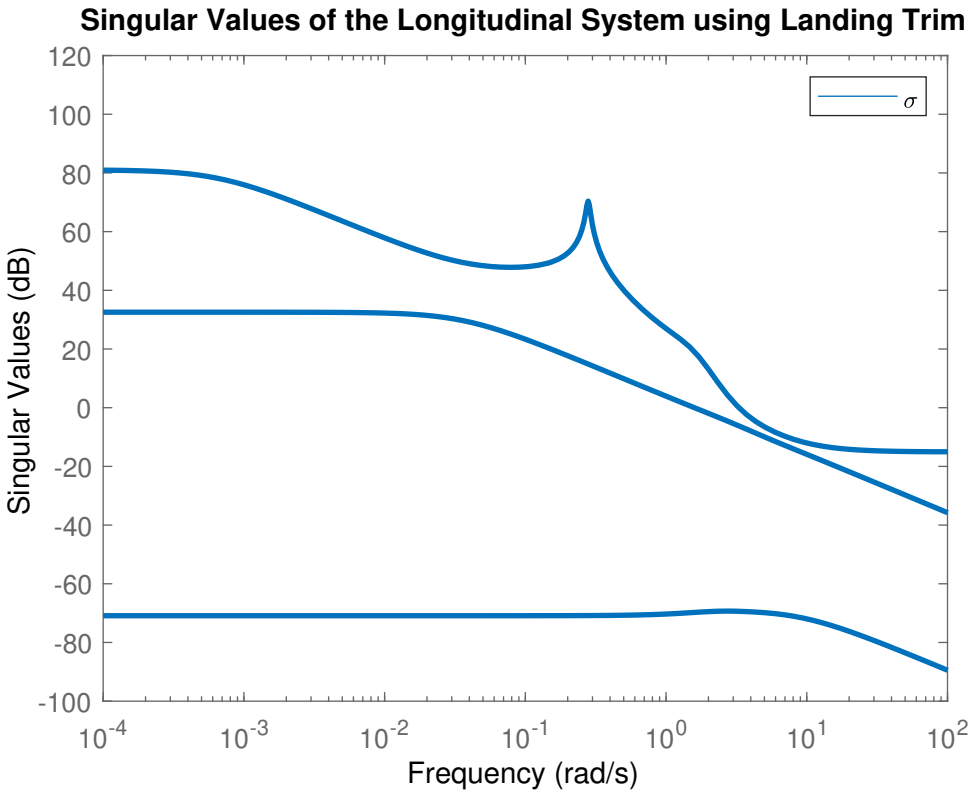

Figure 3.4: Singular value of the longitudinal system around the landing trim point

3.1.6 Pitch Attitude and Plane Geometry

A tailstrike can occur when the aircraft is in contact with the ground but also while airborne in ground proximity. From a pure geometrical viewpoint the pitch value at which it occurs will be dependent on the landing gear's distance to the ground and, in the nonideal case, the tire pressure of the gears. The tire pressure will not be considered. In figure 3.5 a conceptual illustration of the aircraft rear is shown, depicting the angle between the fuselage rear and the ground θ_{strike}.

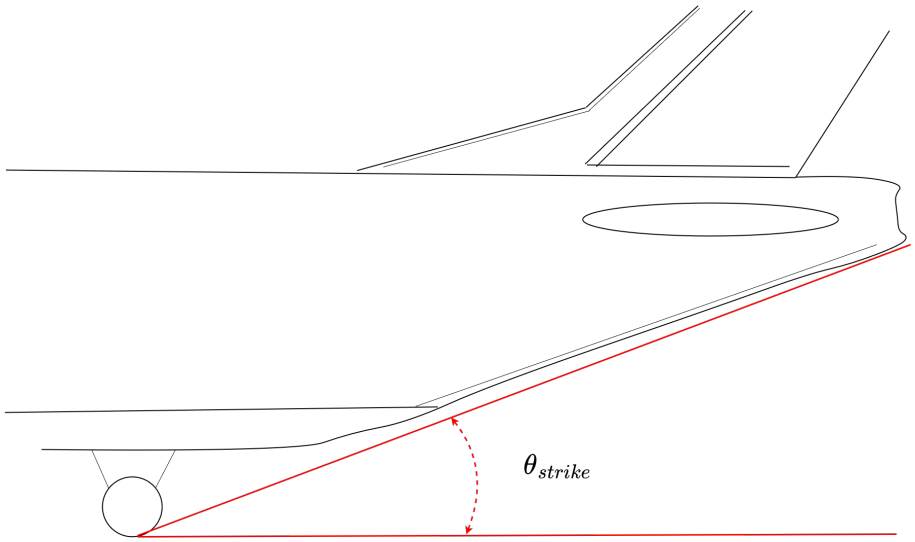

Figure 3.5: Conceptual illustration of the tail angle

By analyzing the aircraft's geometry it could be concluded that a tailstrike incident would occur at a pitch angle of about 14.7° under nominal conditions, standing on the ground.

3.2 Controller Design

In this section the method for designing the controller(s) will be described. The modeling has a defining impact on the control design and thus the controller will be based on the results in 3.1. The flowchrt of the controller and plant structure is displayed in Figure 3.6.

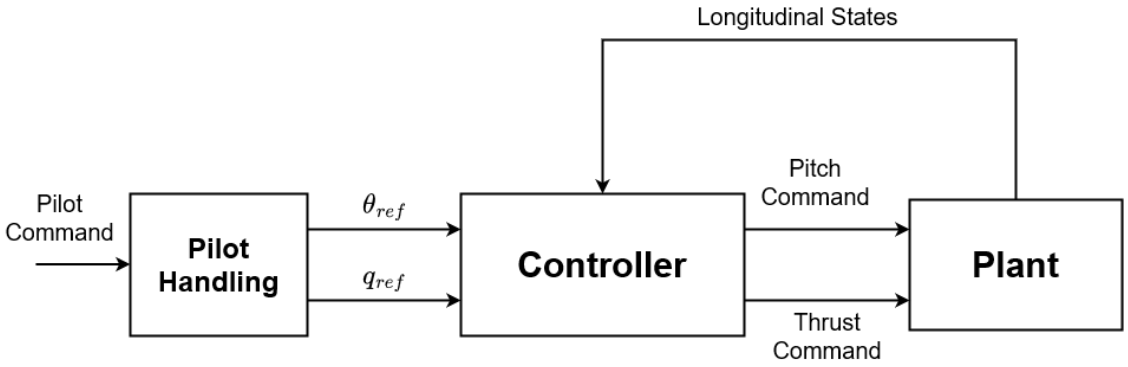

Figure 3.6: Block representation of the controller to the aircraft

3.2.1 Linear Quadratic Regulator

The aircraft model is a system of multiple inputs and multiple outputs (MIMO), and will therefore require a controller suitable for MIMO systems. The linear quadratic

regulator (LQR) is a suitable option. It is easy to implement and has a level of robustness qualities. [14] The controller can make use of integral control to track a pitch attitude reference while simultaneously being designed for inhibiting excessive pitch responses. The LQR is a suitable way to combine the objectives of retaining pilot control through the stick command while still preventing tailstrikes.

In MATLAB the design of the controller can be done using the *lqr()* function. The function takes A, B-matrices together with the control design parameters Q, R, N as input and computes the Riccati equation. The function then outputs the gain matrix K for the optimal state feedback. [24]

Requirements

In order to use a LQR, the linear system must be both controllable and observable. Controllability and observability is computed using the equations 2.30 and 2.31, where each matrix must be of full rank. If a state fails to be controllable, it suffices that the state has a negative eigenvalue. Even if it is not controllable, it can remain stable. [14]

Reference Tracking

In order to incorporate the pilot input into the controller the state-space system needs to be augmented with integral states. Both the pitch and the pitch rate will be used as references, and therefore the system will be augmented with two integral states. The references will be the pilot's means to inform the control system of the desired attitude. The augmented state-space system can be written as

$$\begin{bmatrix} \dot{x} \\ \dot{x}_I \end{bmatrix} = A_d \begin{bmatrix} x \\ x_I \end{bmatrix} + B_d \begin{bmatrix} u \\ u_{ref} \end{bmatrix} \tag{3.6}$$

$$\begin{bmatrix} y \\ e \end{bmatrix} = C_d \begin{bmatrix} x \\ x_I \end{bmatrix} + D_d \begin{bmatrix} u \\ u_{ref} \end{bmatrix} \tag{3.7}$$

where the extended matrices are

$$A_d = \begin{bmatrix} A & \mathbf{0} \\ \mathbf{V} & 0 \end{bmatrix} \tag{3.8}$$

$$B_d = \begin{bmatrix} B & 0 \\ 0 & I_2 \end{bmatrix} \tag{3.9}$$

$$C_d = \begin{bmatrix} C & \mathbf{0} \\ 0 & I_2 \end{bmatrix} \tag{3.10}$$

$$D_d = \begin{bmatrix} D & \mathbf{0} \\ 0 & \mathbf{0} \end{bmatrix} \tag{3.11}$$

The vector V is a vector of two rows with entries on the pitch θ and the pitch rate q. Together with the reference input this will construct the error states $\dot{x}_I$.

$$V = \begin{bmatrix} ... & -1_\theta & ... & 0 & ... \\ ... & 0 & ... & -1_q & ... \end{bmatrix} \tag{3.12}$$

The two approaches are summarized in Table 3.10 with a clarification of the states, the dimensions, the variables to follow and the error state to be minimized.

Reference	**Dimensions**	**Variable**	**Minimizes**
Attitude	rad	θ_{ref}	Steady state error θ_e
Rate	rad/s	q_{ref}	Steady state error q_e

Table 3.10: The two approaches to reference tracking

Pilot Handling

For the controller to incorporate the pilot input, the pilot's command must be converted to an actual pitch attitude or rate for the controller to follow. Therefore, the normalized pilot command must in some way be mapped to an attitude.

The references that are being fed to the controller are calculated in accordance to figure 3.8. The pilot gives a positive or negative command which is intended to emulate a certain elevator deflection. The pilot command-to-elevator gain is a function of the ratio between speed and stall speed V_∞/V_s, center of gravity along the longitudinal plane x_{cg}, and the flap position. In Figure 3.7 the pilot command-to-elevator gearing gain is plotted for $x_{cg} = 0.33$, V_∞/V_s, and the four different flap positions.

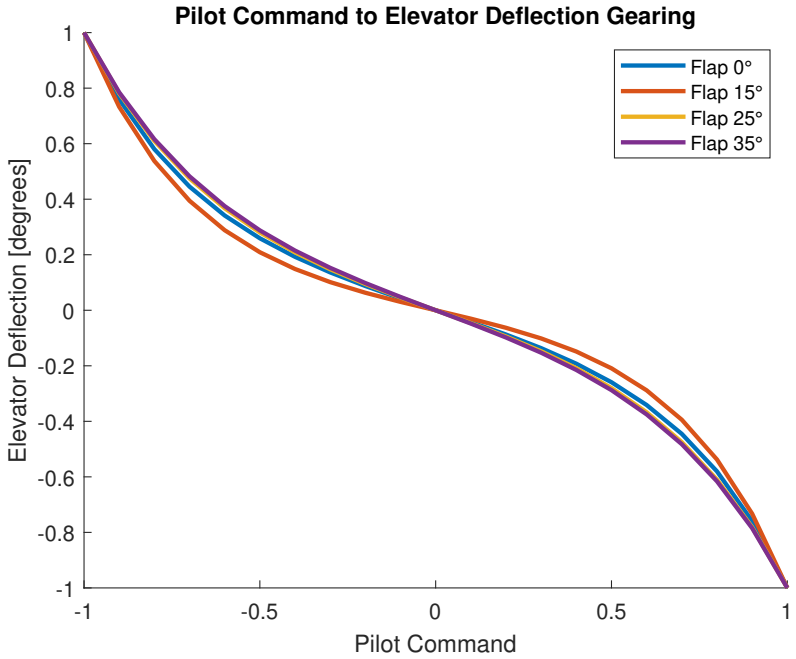

Figure 3.7: Pilot command-to-elevator deflection gearing

The emulated elevator deflection is in turn multiplied with a gearing gain, and for the pitch reference only it will also be integrated over time. The function will output a pitch attitude and rate in radians and radians per second, respectively.

The transfer function from pilot stick command to reference is denoted $G_{q_{ref}}$ or $G_{\theta_{ref}}$ (depending on the reference). The function $f(u_{gear})$ denoted the pilot command to elevator gearing shown in Figure 3.7

$$\frac{G_{q_{ref}}}{f(u_{pilot})} = 4 \cdot \frac{2\pi}{360} \qquad (3.13)$$

$$\frac{G_{\theta_{ref}}}{f(u_{pilot})} = \frac{4}{s} \cdot \frac{2\pi}{360} \qquad (3.14)$$

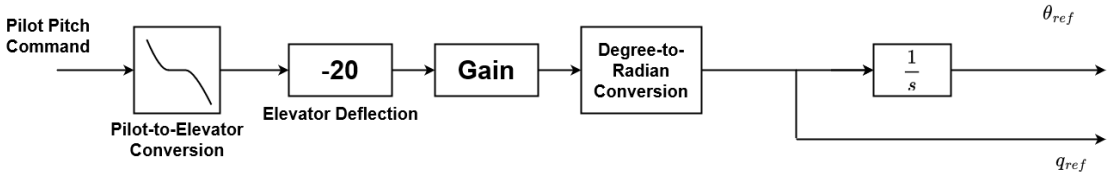

Figure 3.8: Pilot command-to-reference signal for controller

Controller Synthesis

The linear quadratic regulator is a state feedback controller, using the states of the aircraft to construct a control signal through a feedback gain.

One option is to simulate the linear states alongside the nonlinear states if they're not reliable or accessible, and then feed the linear states to the controller. This causes problems if the linear model becomes inaccurate over time.

The other option is to feed the nonlinear states to the controller. The nonlinear states are in this case accessible and appropriate to use. Linear controllers are appropriate to use if the nonlinear dynamics are slow-varying in nature. [14] The control signals computed through K are then connected to the elevator and the four thrust actuators, closing the loop.

Anti-windup

A linear quadratic regulator tracks the reference by minimizing the error state over time. The error state naturally increases as long as the state in question does not match the current reference signal.

In real applications the control signal is oftentimes bounded, and this has implications for the control design. When the controller attempts to reach the reference signal but is restricted by the control signal being saturated, the built-up error (without additional measures) will still continue to increase. [35]

The problem arises when the reference changes, or switches sign. For this new reference value the error state will be incorrect, and the controller will need to wait for the state to wind-down before being able to compute a correct control signal for the given reference. This causes the controller to have a unneccessary long settling time. The control signal might even continue to saturate, due to the build-up in the error state alone. In the cases of disturbances this can cause extreme controller responses and overshoots. [35]

To mitigate this problem the controller will be augmented with an anti-windup technique based on back-calculation. With back-calculation, the difference between the saturated and unsaturated control signal multiplied by a constant will be fed back into the error state, reducing it. [35] The error state are modified according to equations 3.15-3.16

$$\bar{u} - u = 0 \qquad \dot{x}_I = r - y \tag{3.15}$$

$$\bar{u} - u > 0 \qquad \dot{x}_I = r - y + k(\bar{u} - u) \tag{3.16}$$

where $\bar{u}$ is the bounded control signal u, according to

$$\bar{u} = \begin{cases} u & \text{if } -1 \leq u \leq 1 \\ 1 & \text{if } 1 < u \\ -1 & \text{if } u < -1 \end{cases} \tag{3.17}$$

Tuning of Design Parameters

The premise of the linear quadratic regulator is to minimize the cost function and compute an optimal feedback gain. However, what is regarded as *optimal* is a

question of design and desired performance. The design is performed by choosing a Q and R that satisfies the performance objectives of the controller.

The primary states of interest is the pitch θ, the pitch rate q, and their two references θ_{ref} and q_{ref}. The velocity V_x and the height z_e aren't the primary drivers behind a tailstrike and are therefore not of interest in the tuning process. The cost expression for each state are presented on the diagonal of Q in Equation 3.18.

$$Q = \begin{bmatrix} Q_\theta & 0 & 0 & 0 & 0 & 0 & 0 \\ 0 & Q_q & 0 & 0 & 0 & 0 & 0 \\ 0 & 0 & Q_{U_b} & 0 & 0 & 0 & 0 \\ 0 & 0 & 0 & Q_{W_b} & 0 & 0 & 0 \\ 0 & 0 & 0 & 0 & Q_{z_e} & 0 & 0 \\ 0 & 0 & 0 & 0 & 0 & Q_{\theta_e} & 0 \\ 0 & 0 & 0 & 0 & 0 & 0 & Q_{q_e} \end{bmatrix} \tag{3.18}$$

Attitude vs Rate Reference Tracking

There are two probable approaches to the tuning of the controller and incorporating the pilot command through the references. The controller can be designed to either follow the attitude reference θ_{ref} and surpress the pitch rate q, or follow the pitch rate reference q_{ref} and surpress the pitch attitude θ.

The two approaches are displayed in Table 3.11. The premise of option 1 is to track the attitude but slow down the aircraft response such that the aircraft manages to land before tailstriking, while the premise of option 2 is to track a rate but surpress the magnitude of the aircraft response such that it never reaches the critical attitude for a tailstrike.

	Reference Signal	Suppress
Option 1	Attitude	Rate
Option 2	Rate	Attitude

Table 3.11: Two approaches to reference tracking

Disturbance Responses

Any aircraft will most likely be subjected to wind gusts and turbulence that affects the controller's performance. In this section the controller will be evaluated on its response to disturbances using multiple different tuning configurations, with particular emphasis on the cost to the control action.

The Dryden turbulence model is a standardized disturbance model used for aircrafts. [23] In this section the disturbance model will be used to evaluate different tuning configurations of the controller, and in particular what effect the magnitude of the control action has on mitigating disturbances. The cost to the elevator control signal $R(1,1)$ will vary between the values 0.001 and 2 for the closed-loop responses.

In Figure 3.9 the response is shown for a open-loop system subjected to a continuous Dryden wind disturbance. The aircraft is to a beginning relatively steady with a pitch attitude between 2° and 5°, but acquires a sudden negative attitude of $-5°$ at $t \approx 24$ seconds and then pitches up to 10° at $t \approx 35$ seconds. It then levels out at a negative pitch, around -3°. This is the response of the aircraft without closed-loop control action.

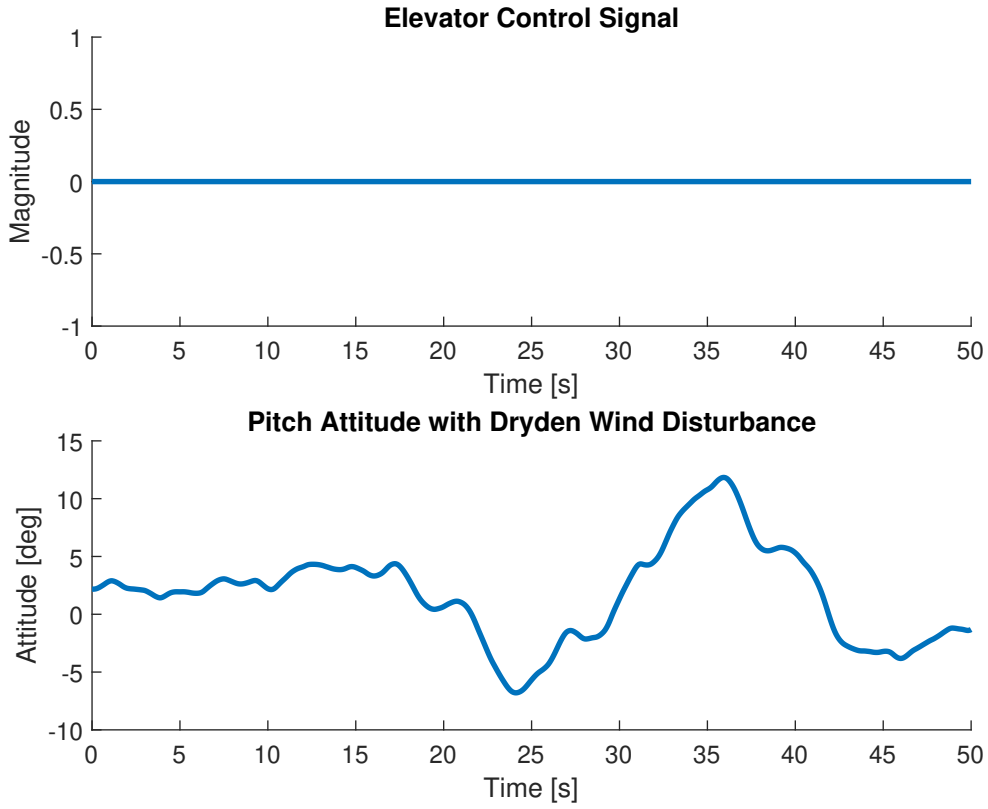

Figure 3.9: Open-loop response to a Dryden wind disturbance

Wind test 1: Attitude Reference Tracking

In the following figures the closed-loop responses are plotted with different tuning configurations. In Figure 3.10 the controller is tuned for following the pitch attitude reference with a cost to the steady state error θ_e, $Q_{\theta_e} = 10$. The tuning to the Q-matrix is then paired with different costs to the elevator control signal $R(1,1)$, where $R(1,1) \in [0.01 \;\; 2]$. The pitch attitude is clearly dampened compared to the open-loop response (see Figure 3.9), staying in the range of approximately 1° to 4° for the worst performance ($R(1,1) = 2$) and between 2° to 2.5° for the best performance ($R(1,1) = 0.01$).

The variances for the control signal and the attitude are presented in Table 3.12. The deviations in pitch attitude from the operating point are lower for a higher control action. A higher control action therefore means a greater resistance to wind turbulence.

R(1,1)	0.01	0.1	0.5	1	2
Var(elevCmd)	0.0026	0.0020	0.0014	0.0012	0.0010
Var(θ)	0.0160	0.0801	0.2281	0.3397	0.4751

Table 3.12: Wind test 1: Variances for elevator command and pitch attitude

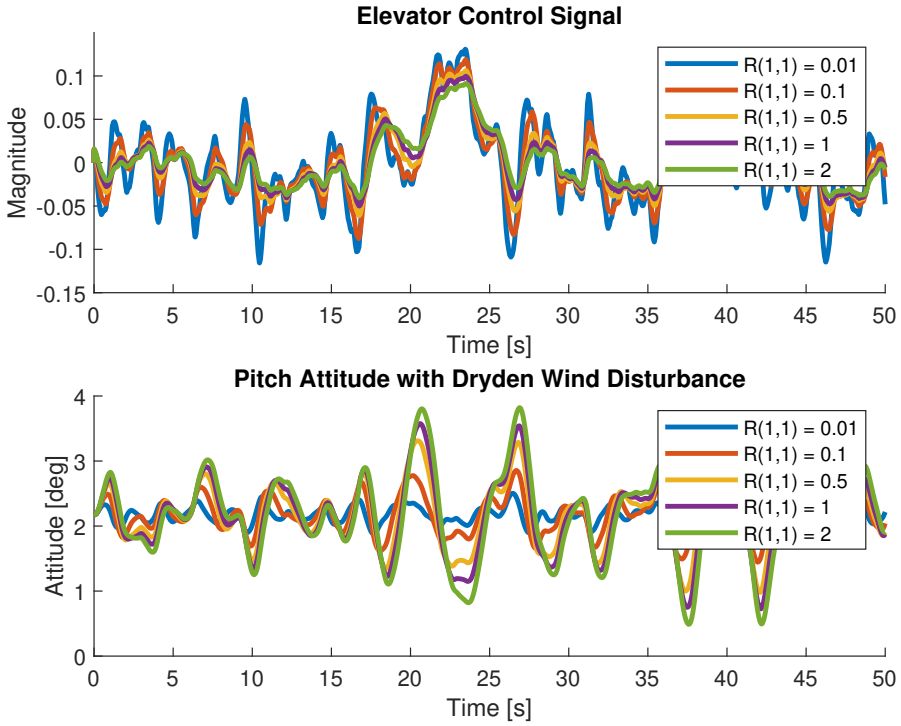

Figure 3.10: Wind test 1: Closed-loop response to Dryden disturbance with $Q_{\theta_e} = 10$

Wind test 2: Attitude Reference Tracking with State Cost

In Figure 3.11 the same cost to the steady state error θ_e is used but with an added cost to the pitch rate q, $Q_q = 5$. As in Wind test 1, the attitude stays within the range 1° to 4° for $R(1,1) = 2$ which is the worst case scenario. For $R(1,1) = 0.1$ the attitude ranges from 2° to 2.5°, but with a heftier control action.

In Table 3.13 the variances are presented for the attitude and elevator control action again. The attitude variance sinks by a factor of 10 from $R(1,1) = 2$ to $R(1,1) = 0.01$. The elevator control action is about the same as in Table 3.12 but the pitch attitude variance is considerably lower. Adding a cost to the pitch rate q improved the mitigation of the Dryden turbulence.

R(1,1)	0.01	0.1	0.5	1	2
Var(elevCmd)	0.0024	0.0020	0.0015	0.0013	0.0010
Var(θ)	0.0030	0.0278	0.1163	0.2003	0.3211

Table 3.13: Windtest 2: Variances for elevator command and pitch attitude

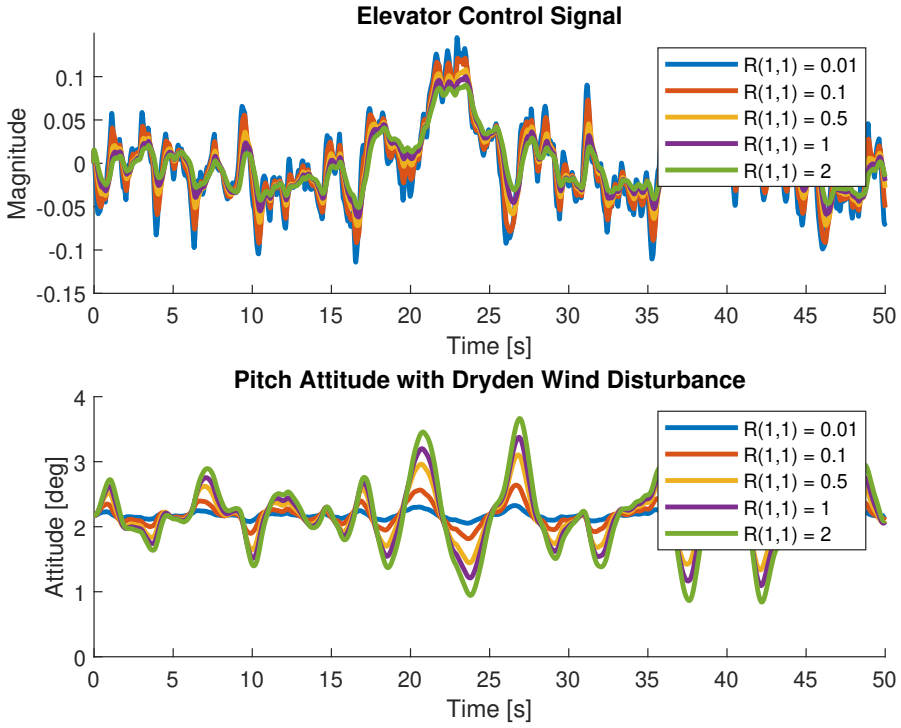

Figure 3.11: Wind test 2: Closed-loop response to Dryden disturbance with $Q_{\theta_e} = 10$ and $Q_q = 5$

Wind Test 3: Rate Reference Tracking

For wind test 3 the controller is tuned for following the pitch rate reference with a cost to the steady state error q_e, $Q_{q_e} = 10$. Figure 3.12 shows that the attitude stays within the range 0° to 4° for $R(1,1) = 2$. A freer control action $R(1,1) = 0.01$ maxes the attitude to about 2.4°.

In Table 3.14 the variances are presented, showing once again that the variance in θ is the lowest for a free control action. Rate reference tracking performs better than the attitude tracking (see wind test 1 3.12) for all values of $R(1,1)$, without a cost to θ or q.

R(1,1)	0.01	0.1	0.5	1	2
Var(elevCmd)	0.0024	0.0018	0.0012	0.0010	0.0008
Var(θ)	0.0073	0.0551	0.1869	0.2949	0.4487

Table 3.14: Windtest 3: Variances for elevator command and pitch attitude

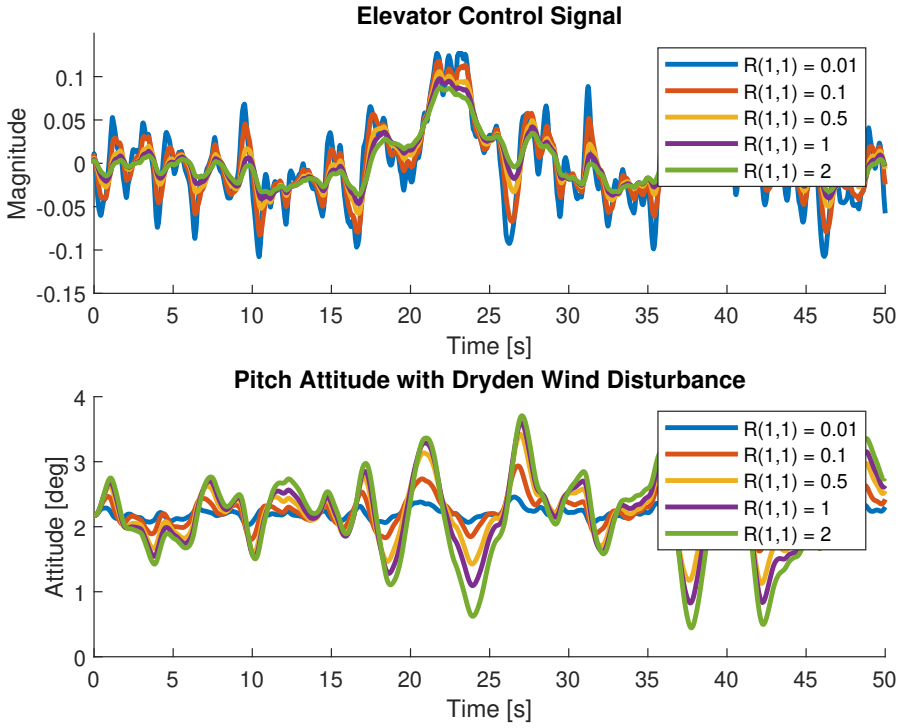

Figure 3.12: Wind test 3: Closed-loop response to Dryden disturbance with $Q_{q_e} = 10$

Wind Test 4: Rate Reference Tracking with State Cost

In wind test 4 the same cost is applied to the steady state error for the rate (Q_{q_e}) as in wind test 3, but with an added cost to the pitch attitude $Q_\theta = 5$. The results are shown in figure 3.13.

The tuning setting dampens the turbulence in this case too, but exhibits a heftier control signal action than without a cost to the state θ. However, the variance does not exceed that of the previous tests for any value of $R(1,1)$. This is shown in Table 3.15. The variance in attitude is now kept to a mere 0.004° deviation for the freest control action.

R(1,1)	**0.01**	**0.1**	**0.5**	**1**	**2**
Var(elevCmd)	0.0024	0.0019	0.0014	0.0011	0.0009
Var(θ)	0.0050	0.0393	0.1401	0.2264	0.3504

Table 3.15: Windtest 4: Variances for elevator command and pitch attitude

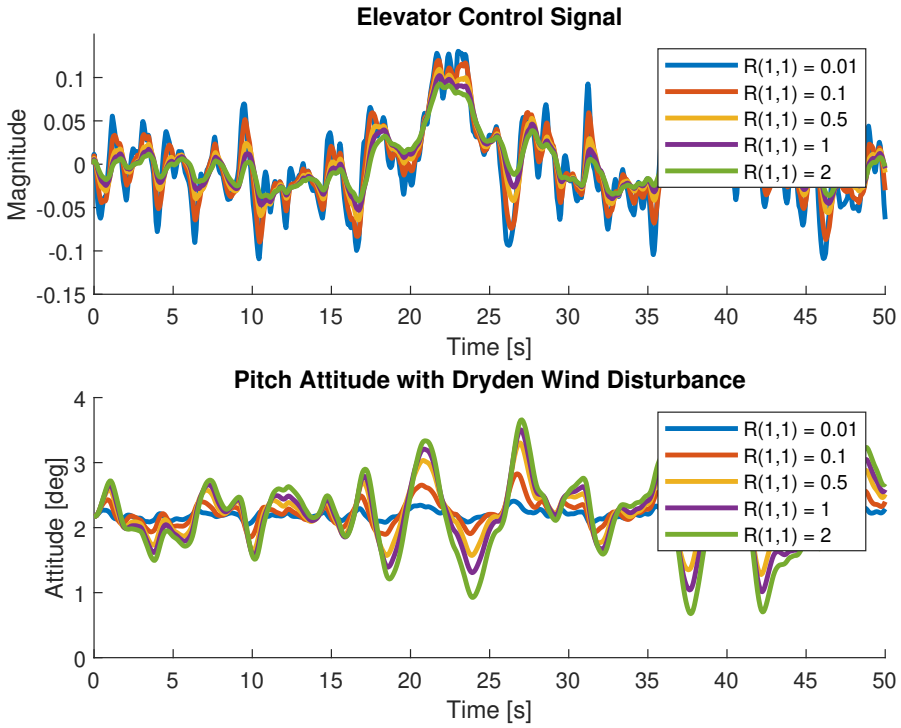

Figure 3.13: Wind test 3: Closed-loop response to Dryden disturbance with $Q_{q_e} = 10$ and $Q_\theta = 5$

The conclusion from the four wind tests is that a free control action of $R(1,1) = 0.01$ has the best performance for all tests. The reaction from the control signal can seem sharp for some tests, but a magnitude of 0.1 corresponds to only a 2° of elevator deflection. This is tolerable.

The costs $Q_{\theta_e} = 10$, $Q_q = 5$ from wind test 2 shows the best performance (lowest variance to θ), however the $Q_{q_e} = 10$ with $Q_\theta = 5$ comes in at a close second with no particular difference.

Frequency Responses

It is of interest to observe the singular values over the frequency range for these two approaches. They tell us how the gains vary over a frequency range and is therefore useful in analyzing the robustness of the system.

In the SISO case phase margins are also used to analyze the stability margins of a system, but in MIMO systems the phase margin of individual signals will not give any useful information about the robustness of a system. [31]

In Figure 3.14 the controller has been tuned for following the pitch attitude reference θ_{ref} (equivalent to minimizing θ_e) and minimizing the pitch rate q, and thereafter plotted over a typical frequency range. The peak magnitude of the open-loop system has disappeared through the state feedback and the gain been reduced to 0 db for frequencies up to $\omega = 1$ rad/s. An increased punishment to the rate q lowers the gain slightly while decreasing the crossover frequency as well. The gains are attenuated for high frequencies.

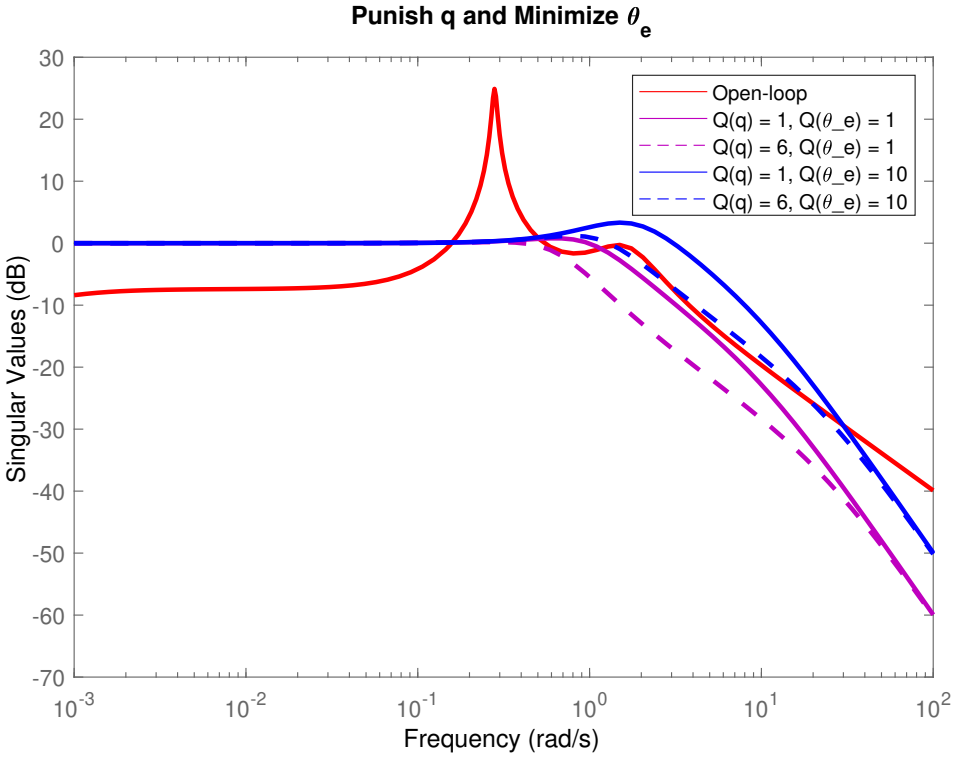

Figure 3.14: Frequency response of closed loop linearized system with suppression of the rate while following an attitude reference

In Figure 3.14 the controller has been tuned for following the pitch attitude reference q_{ref} (equivalent to minimizing q_e) and minimizing the pitch attitude θ, and also plotted over multiple frequencies. This tuning configurations shows a larger sensitivity for lower frequencies than the ones displayed in 3.14. However, the gains can be manipulated by altering the cost $Q(\theta)$, increasing it gives a reduced gain.

The gain is reduced more if the cost to the pitch rate error state q_e is lowered as well, which is observed by comparing the dotted lines to their respective whole drawn lines. There is a larger gap between the purple lines ($Q(q_e) = 1$) than between the

blue ($Q(q_e) = 10$), indicating that the larger the cost $Q(q_e)$ the less effective an increase in $Q(\theta)$ is.

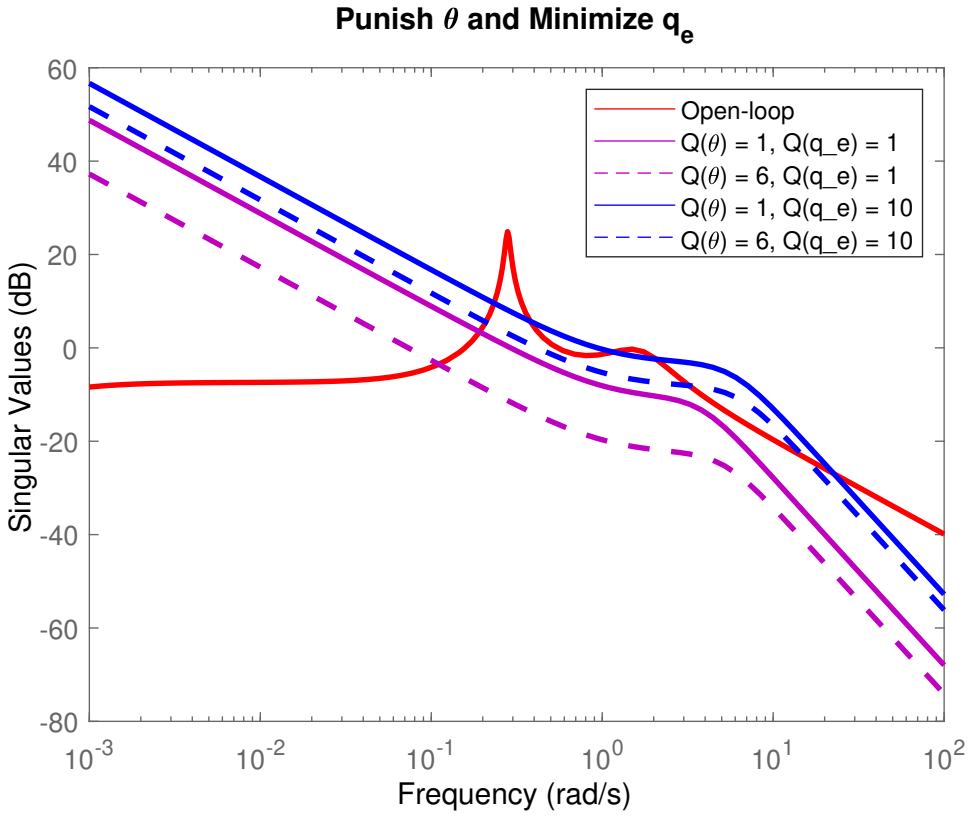

Figure 3.15: Frequency response of closed loop linearized system with suppression of the attitude while following a rate reference

Impulse Command Responses

In section 3.2.1 the motivation behind the reference tracking was explained. The state-space model was equipped with two integral states for reference tracking, one for the attitude and one for the rate.

A tracking on the attitude will be paired with a cost to the rate, and vice versa. The reason for this is that there an evident conflict between tracking a parameter and attempting to apply a cost to the same parameter.

Tracking the attitude versus tracking the rate is expected to yield two different responses. In the following test the cost to the control action is the same in both cases and is presented in equation 3.19. The cost to the elevator command is set to $R(1,1) = 0.01$. This allows for faster aircraft responses and has the best turbulence mitigation performance.

The pilot command is a full pitch-up command over the duration of one second. The pilot command translates into a reference attitude and rate.

$$R = \begin{bmatrix} 0.01 & 0 & 0 & 0 & 0 \\ 0 & 1 & 0 & 0 & 0 \\ 0 & 0 & 1 & 0 & 0 \\ 0 & 0 & 0 & 1 & 0 \\ 0 & 0 & 0 & 0 & 1 \end{bmatrix} \tag{3.19}$$

In Figure 3.16 the results for tracking the attitude is illustrated. The plot depicts the aircraft response for the different tuning configurations beginning with zero cost to the rate for pure tracking, and thereafter proceeding with a cost to the pitch rate q. This will delay the aircraft from reaching the maximum attitude compared to no cost to the pitch rate.

An attempt to both follow the attitude and suppress it was done, with $Q_{\theta_e} = 5, Q_\theta = 5$. This did not affect the resulting attitude at all, it converged towards the reference anyways. It only took a slightly longer time to do so.

From the pilot's point of view a delayed response of this character would risk being too non-responsive. There is also no guarantee that this will prevent the tailstrike. The pilot should still feel in control of the aircraft, in particular if another, more dire situation arises during the landing operation.

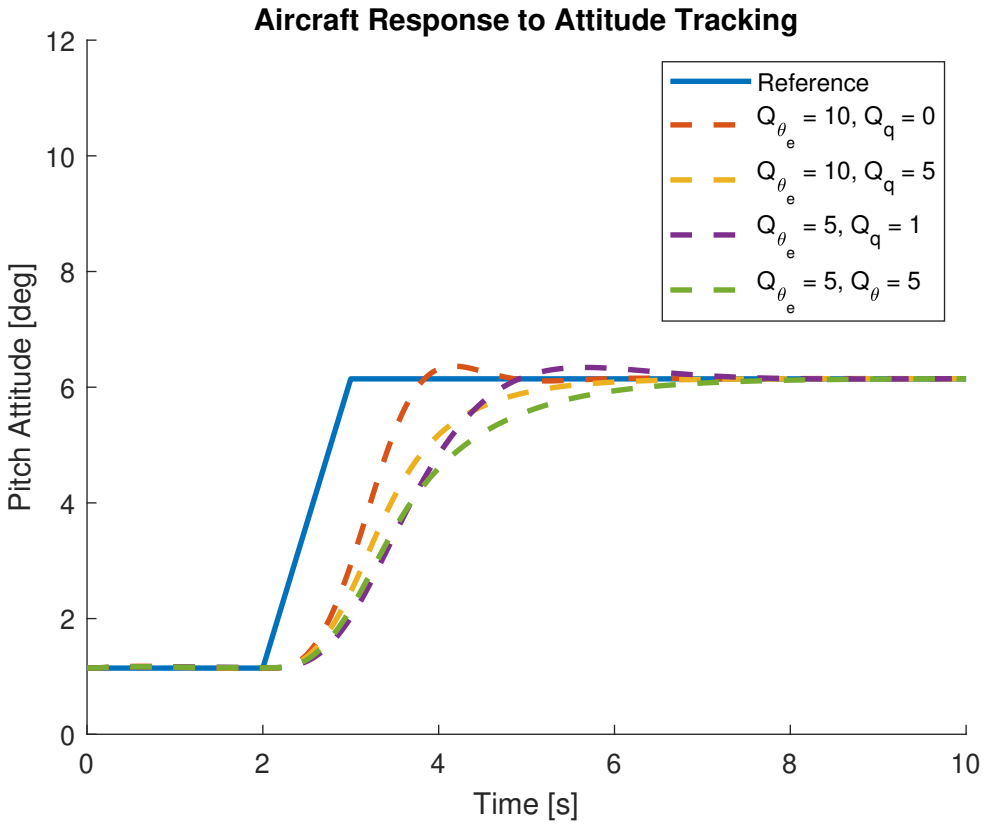

Figure 3.16: Aircraft response to tracking an attitude, with different costs to the pitch rate.

In Figure 3.17 the results for the pitch rate tracking are presented, also illustrating the aircraft response with different tuning parameters. An observation is that pure rate tracking generates a steady state error to the attitude reference. This is not a concern as this approach does not attempt to do so.

The cost to the pitch attitude has a clear effect on the magnitude of the response. A cost of $Q_\theta = 5$ decreases the attitude by about 2.7° compared to a cost $Q_\theta = 0$ for a maximum pilot command at a duration of one second. Lowering the cost to the pitch rate's error state θ_e can lower the achieved attitude even more.

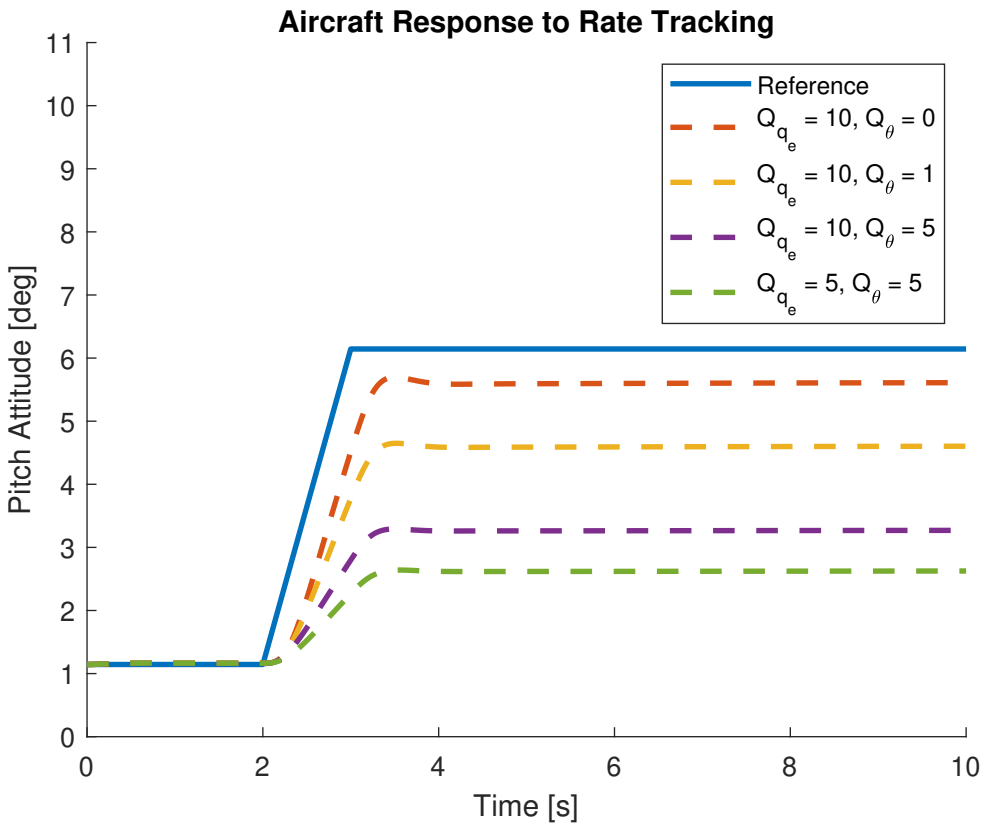

Figure 3.17: Aircraft response to tracking the rate of the pilot command, with different costs to the pitch magnitude.

3.2.2 Summary and Analysis of Single-Gain Tuning

In this section the observations from the tuning process in the previous sections are summarized.

- Tracking the attitude reference θ_{ref} while applying a cost to the rate θ is a poor solution to preventing a tailstrike. Attitude tracking can generate large steady-state errors which if left unchecked can generate unpredictable controller actions, and simply delaying the response of the aircraft through a cost to the rate θ is not a reliable preventive measure.

- Tracking pitch rate reference θ_{ref} and applying a cost to the attitude θ is the preferable approach. Regulating the pitch state in this manner has a clear effect on the aircaft's ability to overrotate, suggesting that this is a stable approach to preventing a tailstrike. This will be the approach forward.

- There is a natural conflict between tracking a pitch command from the pilot while simultaneously attempting to dampen it through the same control signal. A responsive aircraft will come with the cost of poor tailstrike-preventive abilities, while good preventive abilities will give a less responsive aircraft during flight.

- Raising costs on the error state θ_e and the dynamic states simultaneously up to $\approx$ 8-10 will increase the risk for instability or unpredictable behaviour.

- Large gains and non-restrictive elevator control signal gives a controller that is very effective at mitigating wind turbulence. A free control action gives a more stable aircraft in the case of turbulence.

From the listed observations above it is apparent that there are conflicting objectives in the tuning of the controller when using a single state feedback matrix. One single tuning cannot satisfy all objectives during the span of a landing or takeoff operation.

A solution to this problem is to switch between feedback gains depending on a schedule. With this approach the controller can be tuned for giving the pilot full control over the aircraft when the risk for tailstrike is low, but undermine his commands when the aircraft reaches the critical pitch attitude θ_{strike}.

3.3 Gain Scheduling

The methods described in sections 3.1 and 3.2 has primarily revolved around using a single operating point to linearize around and design a controller for. There are two drawbacks to this approach.

The obvious drawback is that the controller will be based on an operating point that no longer applies when the flight conditions change, even if the controller has some robustness properties.

The second drawback is described in subsection 3.2.2 - a single gain cannot fulfill the multiple different objectives that the controller has over a full landing or takeoff operation.

A suitable approach is to use gain scheduling. With gain scheduling multiple gains K are computed and switched between depending on certain flight condition parameters. These gains reflect the current dynamics more accurately [31] and allows for different tunings of the controller at these different flight conditions.

The downside with gain scheduling is that any closed-loop properties can only be

concluded close to the specific operating point of which the gain is based on. [7] Hence a considerable amount of simulation and testing is neccessary to guarantee safe performance and predictable behaviour for the whole flight envelope.

3.3.1 Batch Trimming and Linearization

To implement a gain schedule multiple operating point must be computed using batch trimming and linearization. Since the risk for tailstrike is dependent on the pitch attitude and the speed of the aircraft, the pitch attitude θ and the true airspeed (TAS) are selected as scheduling parameters for the trim.

Ideally the equivalent airspeed (EAS) should be used, as it does not change with temperature or wind gusts, but it is not available as a trim setting. However, it will be used as the scheduling parameter for the gains in place of the true airspeed, to avoid a scheduling dependent on tempature and wind fluctuation.

Additional scheduling parameters can be used, such as altitude H_m and load factor n_z, but in this thesis the scheduling parameters are limited to two. Trimming for the flight path angle γ would be appropriate, but because of the flight path's direct relationship to the pitch attitude (see equation 2.4 it would overconstraint the trim. This would cause the trim to fail a majority of the cases.

In Table 3.16 the parameter range for the two scheduling parameters are presented with a minimum and maximum value. The batch trimming iterates through each value and attempts to trim for the specific setting. The model trims for the attitude using the stabilizers, and the thrust level is unconstrained.

	Min	Max	Number of points
θ	3°	14 °	12
TAS	44 m/s	60 m/s	17

Table 3.16: Grid for the operating points based on θ and TAS

Figure 3.18 depicts the operating points on a grid for each value of θ and true airspeed (TAS) of the aircraft. The blue points in the figure represents operating points where a trim was successful, and the red dots represents the points at which it was unable to trim.

Its is worth noting that there might exist solutions at the red points for other trimming options or constraints. It is likely an issue of the optimization algorithm converging towards a local minima that fails to meet the constraints. To find a solution for these dots a different optimization method could be used, but since a large amount of the trims were succesful the batch can be used.

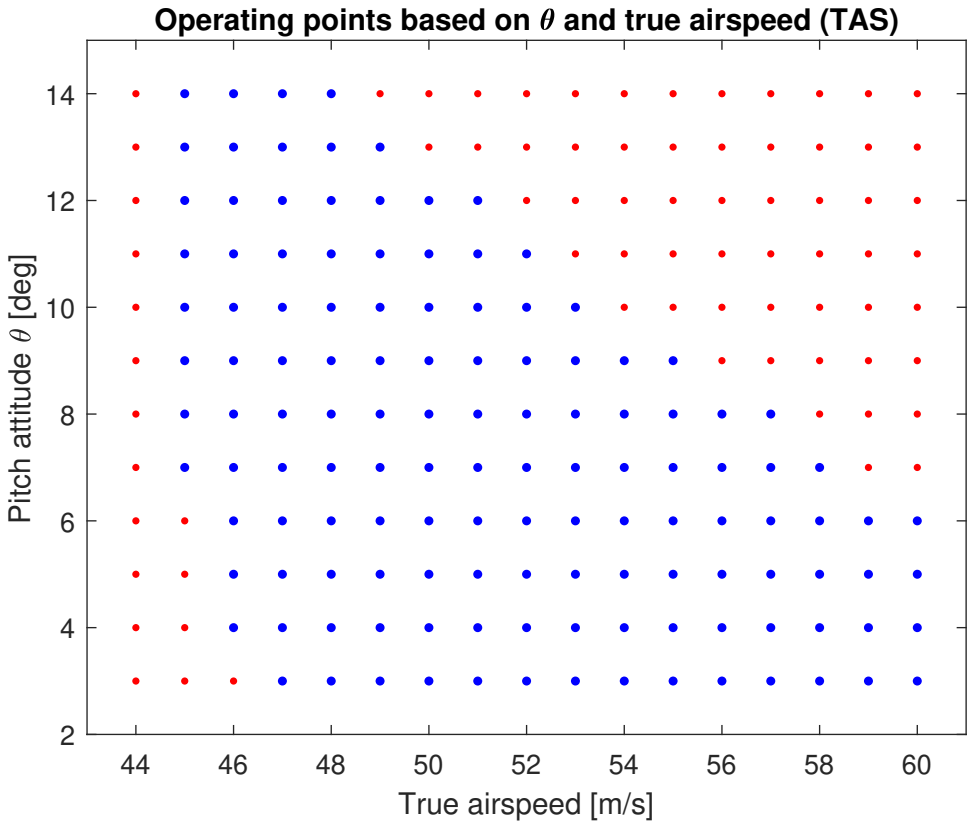

Figure 3.18: Polytope of the nonlinear aircrafts

In Figure 3.19 the pole-zero map for the longitudinal dynamics is plotted for the whole polytope. The poles are colored dependent on the airspeed in the scheduling range, ranging from low (green) to high (red). From the figure it can be observed that the placement of the poles, and therefore the stability, is dependent on the true airspeed of the aircraft rather than the attitude θ. It shows that the aircraft response for a elevator doublet, the short period, becomes more stable for higher airspeeds. The phugoid mode however becomes less stable for higher airspeeds. For some midrange airspeeds the dynamics even become unstable.

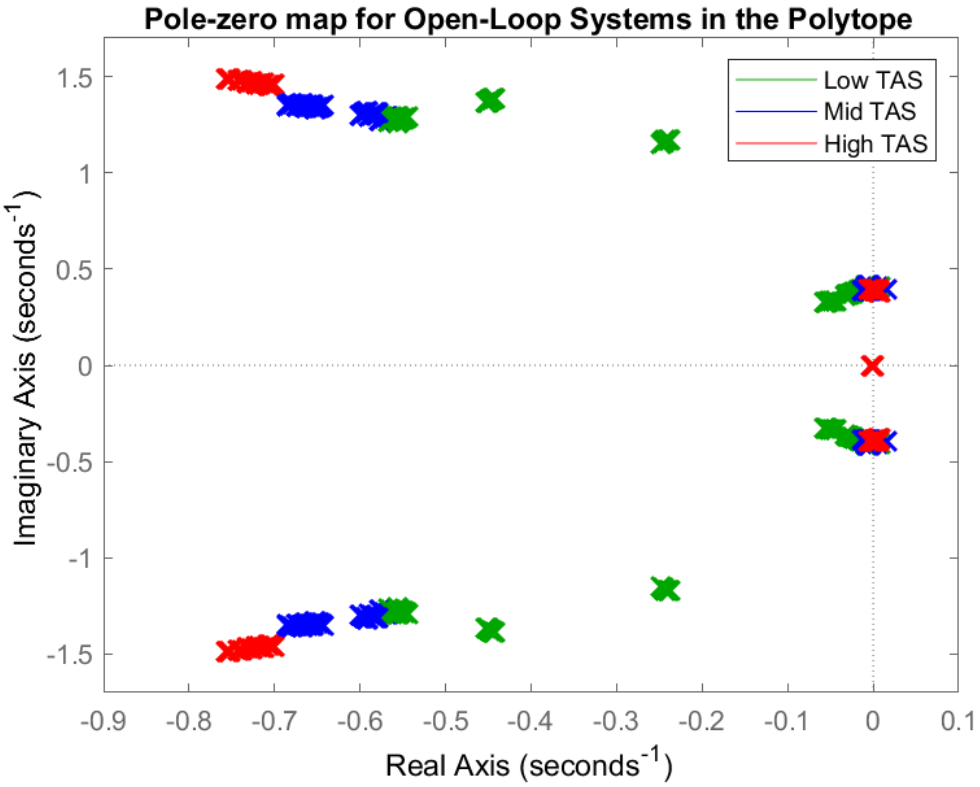

Figure 3.19: Pole-zero map for the longitudinal dynamics over the whole polytope for the systems in open-loop

3.3.2 Gain Switching and Interpolation

The state feedback gains K are computed from one single operating point each, and are to be scheduled between based on the scheduling parameters. In order to avoid discrete switches when the scheduling parameters reaches a new integer value, interpolation is used. The resulting feedback gain will then be a mixture of the four closest feedback gains on the grid. This is a two-dimensional interpretation of linear interpolation that is also suggested in [7]. The formula used for interpolation reads

$$K_{\text{TAS},\theta} = (1-a)(1-b)K_{1,1} + (1-a)bK_{2,1} + a(1-b)K_{1,2} + abK_{2,2} \tag{3.20}$$

where a and b are equal to the current parameter values subtracted by its' floor values $\underline{\theta}$, $\underline{\text{TAS}}$. This also equals the fraction of the ceiling value.

$$a = \theta - \underline{\theta} \qquad 0 \leq a < 1 \tag{3.21}$$

$$b = \text{TAS} - \underline{\text{TAS}} \qquad 0 \leq b < 1 \tag{3.22}$$

In Figure 3.20 the interpolation method is illustrated for a pair of scheduling parameter values (TAS, θ). The attitude is plotted on the y-axis and the true airspeed

is plotted on the x-axis. The feedback gain $K_{\text{TAS},\theta}$ is computed as a percentage of each adjacent feedback gain.

Recall that for some pairs of (TAS, θ) the trimming algorithm could not find valid operating points (see figure 3.18), and consequently no feedback gains can be produced for these pairs. When the scheduling parameters exits the region of which there exists operating points, the last computed feedback matrix will be used until the parameters re-enters the valid parametric region.

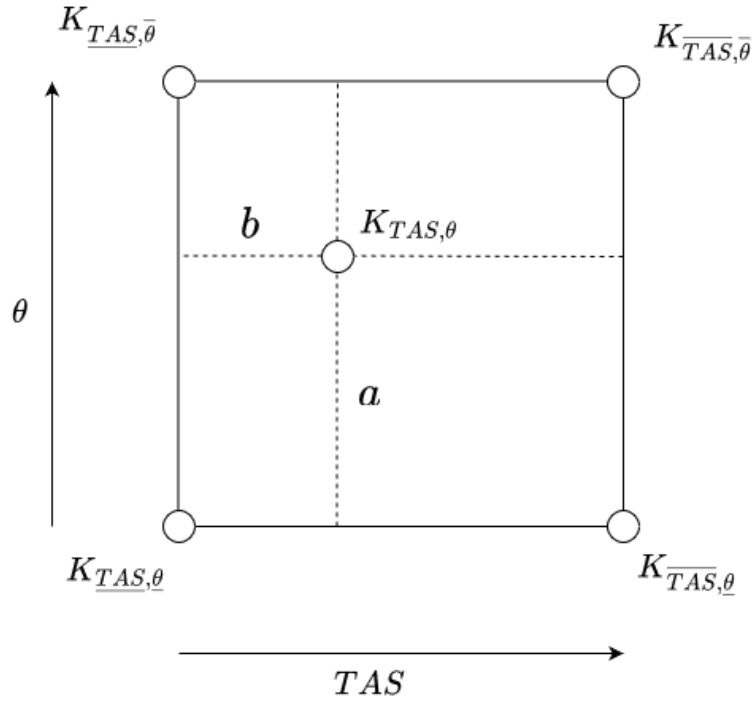

Figure 3.20: Gain interpolation

3.3.3 Schedule-Dependent Tuning

The tuning schedule will be designed according to two objectives.

- Allow the pilot full control of the pitch attitude when the risk for tailstrike is low or none
- Counteract the pilot's pitch-up command when approaching the critical attitude for a tailstrike

To fulfill the two objectives the cost to the steady state error q_e should be high at low attitudes and steadily sink towards higher attitudes. On the opposite side, the cost to the pitch attitude θ should be low at first and increase when the atitude approaches θ_{strike}.

In Figures 3.21 and 3.22 the five different cost schedules are presented for the tests

(see next section about Flight Simulator Testing, 3.4), where the cost Q_θ is increased incrementally as a function of θ. The cost schedules are categorised as Easy/Medium/Tough/Tougher, which refers to the steepness of the cost increase. Rather than increasing the maximum cost the costs becomes higher *sooner*.

The cost to the steady state error Q_{q_e} is identical for cases 1-4. It is decreased to lower the pilot control and reduce the feedback gain. Case 5 is designed to put even more emphasize into the responsiveness at low attitudes and applying a higher maximum cost at higher attitudes than cases 1-4.

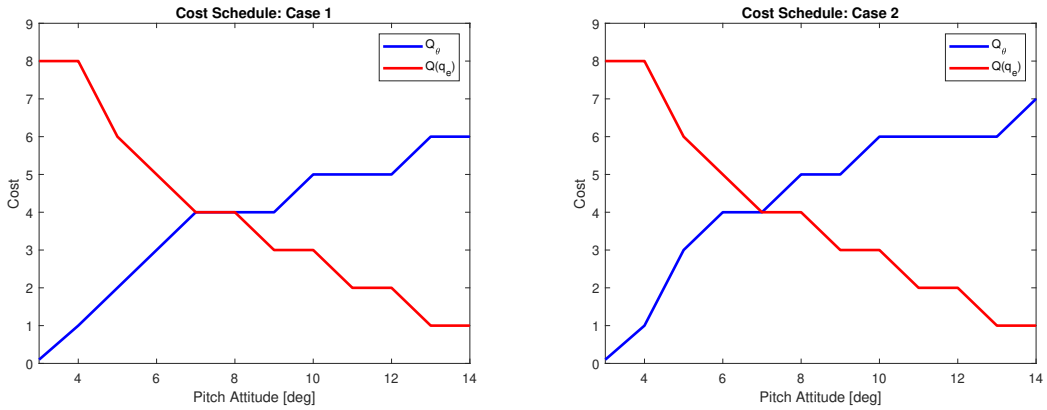

Figure 3.21: a) Cost schedule for Case 1: Easy, b) Cost schedule for Case 2: Medium

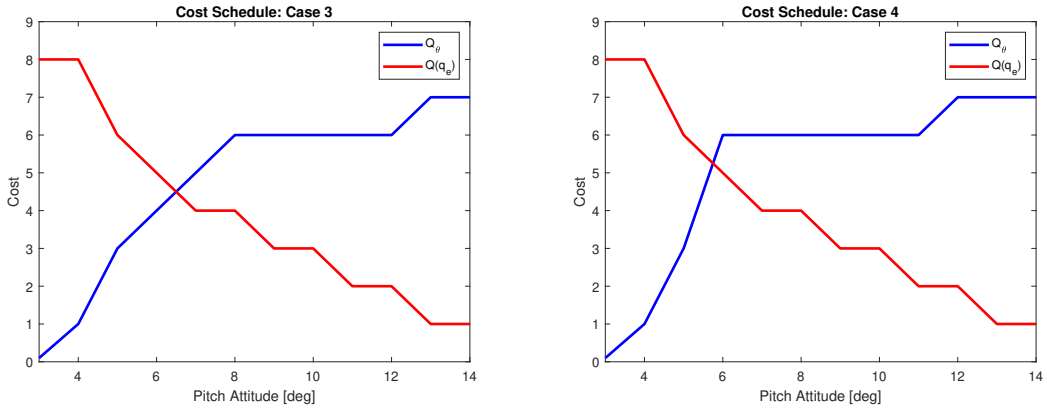

Figure 3.22: a) Cost schedule for Case 3: Tough, b) Cost schedule for Case 4: Tougher

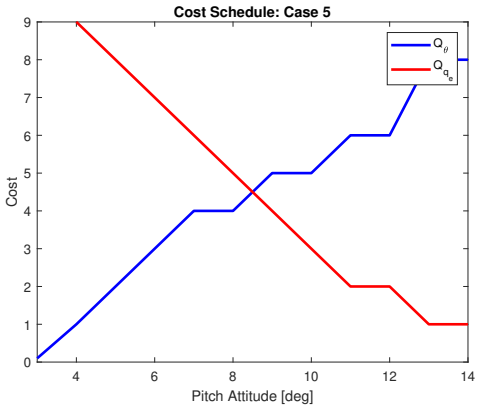

Figure 3.23: Cost schedule for Case 5: Medium

In Figure 3.19 the pole-zero map for the longitudinal dynamics is plotted for the whole polytope, but for a closed-loop system with the feedback gains K based on the first cost schedule, case 1. The feedback moves the phugoid poles more to the left in the plane compared with the open-loop system, showing that the aircraft in a closed-loop system will return to the trimmed position without problem. By observing that the phugoid poles are zero-valued on the imaginary axis one can conclude that the oscillatory behaviour is either none or reduced.

The short period poles are also more stable than in the open-loop systems, and are increasingly more stable for higher airspeeds.

The closed-loop poles with the other cost schedules are similar, and pole-zero plots for those closed-loop systems are therefor omitted. The poles for the other closed-loop systems are only slightly shifted.

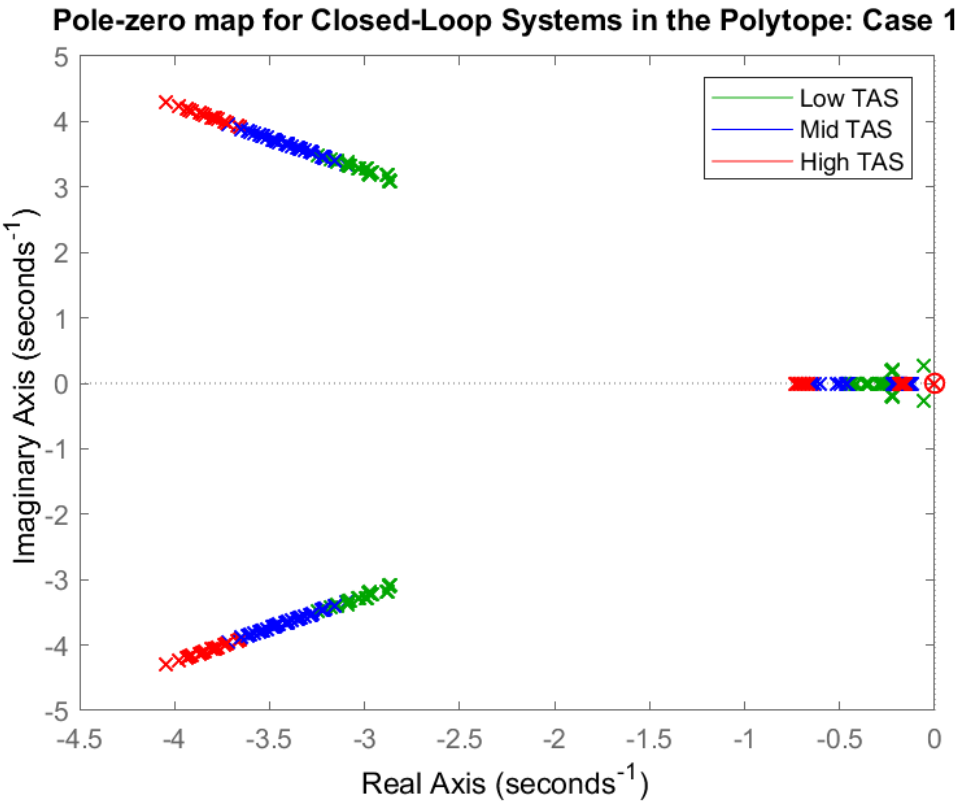

Figure 3.24: Pole-zero map for the longitudinal dynamics over the whole polytope for the systems in closed-loop, using gains based on cost schedule Case 1

The pole-placement of closed-loop systems can be informative for the specific operating points, but the poles are not certain to stay when the model is perturbed. [6] To assess the robustness the singular values of the closed-loop systems for the most edge flight conditions in the polytope are plotted in Figure 3.25 and 3.26. Here edge flight conditions refer to flight conditions for the minimal and maximal values possible for the scheduling parameters, such as $\theta = 14°$ and TAS= 60 m/s. The tuning used for the closed-loop systems is the case 1 cost schedule.

The transfer function from the input to the reference is included. G_{pilot} is here assigned

$$G_{pilot} = G_{q_{ref}} \tag{3.23}$$

The singular values are plotted from the input reference q_{ref} to the pitch attitude θ and rate q. The open-loop systems all have a gain $\sigma < 1$ for the low and high frequencies, and only have a gain above 1 for frequencies in the approximate range $0.2 < \omega < 1.2$ rad/second with a peak magnitude at about $\omega \approx 0.4$.

The closed-loop systems suppresses the peak responses in all cases but have very

high gain for low frequencies. This indicates a high sensitive controller. It is also not strange that a low frequency signal, such as a prolonged pilot command in the form of a sinewave, will generate high gains if it is integrated over time. It is more important that high frequency signals are attenuated to prevent wind turbulence.

With the transfer function from the pilot stick command to the reference command G_{pilot} (see section 3.2.1) included the gain decreases more, such $\omega < 1$ for a wider range of frequencies. It is more relevant to keep the gain around 1 for $\omega \approx 0.1 - 1$ since this is the likely frequency range of the pilot stick commands.

Note that the gain is the lowest for $\omega = 1$ at the operating point with $\theta = 14°$ and TAS $= 45$ m/s, which indicates that the punishment to the attitude is the largest at this point.

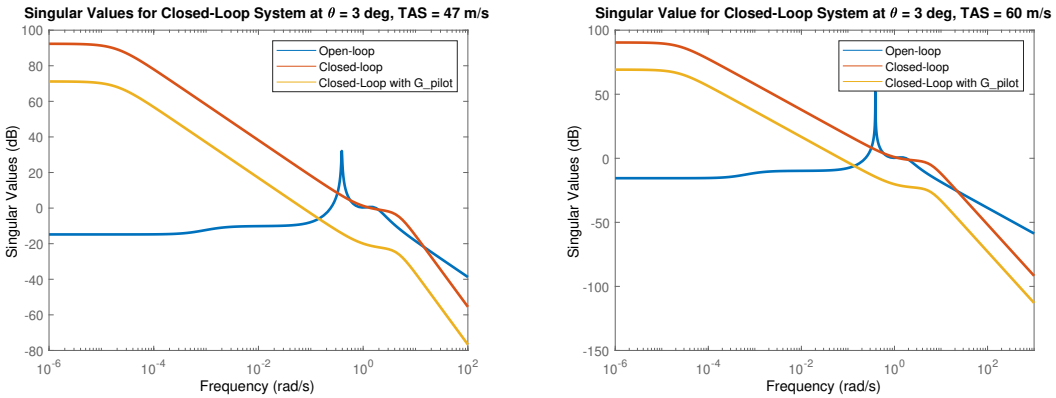

Figure 3.25: Singular values for low-atiitude flight conditions

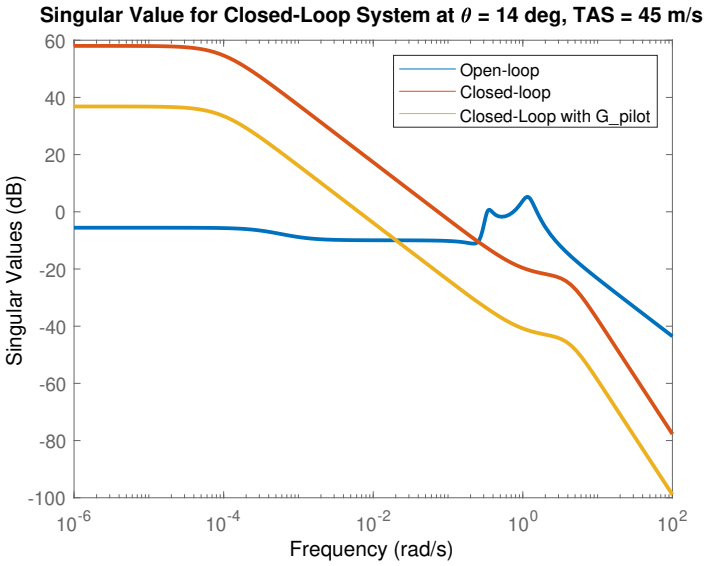

Figure 3.26: Singular values for high-attitude flight conditions

3.4 Flight Simulator Testing

To test the controller(s) tailstrike prevention abilities, a pilot will be instructed to perform multiple takeoffs and landings in the flight simulator. The aircraft will be aligned with the runway. When the aircraft approaches the runway the pilot will flare up prematurely before touchdown.

Since common causes of tailstrike during the takeoff phase is rotation at improper speed and excessive pitch rate, two types of test were preformed. Firstly one at which V_r is reached followed by the pilot giving the maximum pitch command. Secondly one where the pilot starts the rotation before V_r is reached.

The pilot will perform the operations in both open-loop and closed-loop, with single-gain and with gain scheduling, and with multiple different tunings ranging from a easy to a tough tuning. The tests will be randomized to prevent bias, and the pilot will not be informed of the controller tunings.

The tests are presented in Table 3.17.

Test	**Type**	**Level of Control**	Q_θ	Q_{q_e}
Test 1	Open-loop	None	0	0
Test 2	Single-Gain	Low	0	10
Test 3	Single-Gain	Low	1	10
Test 4	Single-Gain	Medium	3	8
Test 5	Single-Gain	Tough	5	6
Test 6	Schedule	Low	Case 1	Case 1
Test 7	Schedule	Medium	Case 2	Case 2
Test 8	Schedule	Tough	Case 3	Case 3
Test 9	Schedule	Tougher	Case 4	Case 4
Test 10	Schedule	Medium	Case 5	Case 5

Table 3.17: Tests for the flight simulator

4

Results

4.1 Flight Simulator Testing

In this section the results from the flight simulator testing with the pilot is presented. The results are divided up into the landing tests and the takeoff tests.

4.1.1 Landing

The settings for the tests are presented in Table 3.17 and the method for testing is described in subsection 3.4. In the following Figures the single-gain results are presented on the left, and the scheduled gain results are presented on the right.

In Figure 4.1 the attitude for each test is displayed. In Figure 4.1a the attitude exceeds the critical attitude $\theta_{strike} = 14.7°$ for three out of four cases with the single tuning. For test 2 and 3 this is not unexpected, since in the first test there is no cost to the attitude ($Q_\theta = 0$) and in the second the cost is very low ($Q_\theta = 1$). The tailstrike preventive abilities of these controller tunings are none to low. The cost to the pitch state is potent first in test 4, but a tailstrike still occurred. It was first in test 5 a tailstrike was prevented with a single gain.

In Figure 4.1b the attitude exceeds the critical attitude $\theta_{strike} = 14.7°$ for none of the tests, preventing a tailstrike for all five tuning schedules. In general, the more aggressive the tuning case, the lower the achieved pitch is at touchdown. The exception is for test 9, where the pilot flares for a duration of $t \approx 15$ seconds. This deviates from the average flare duration of the other tests, $t \approx 9$ seconds. Because of the longer flare the aircraft is able to achieve a higher attitude, however, this still does not produce a tailstrike.

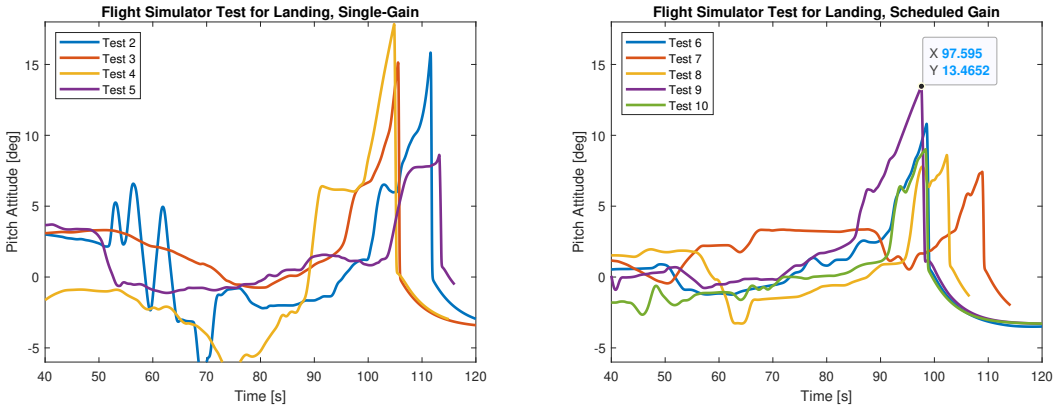

Figure 4.1: Pitch attitude for landing with a) single-gain b) scheduled gain

A common comment from the pilot performing the tests was the low responsiveness, and an important quantity to measure responsiveness is the pitch rate q. In Figures 4.2 the pitch rates q of the aircraft for each test is displayed. For the single-gain tests the maximal pitch rate had a clear correlation to the pitch cost Q_θ. The rate could reach the highest values of ± 5 deg/second for $Q_\theta = 0$ (the rate ± 5 deg/second is the maximal rate the reference could reach with the current gains settings for the pilot command), decreasing to ± 4 deg/second for $Q_\theta = 1$ and to ± 1.7 deg/second for $Q_\theta = 5$.

The scheduled gains were percieved as a little more responsive than the tunings in the single-gain tests. The pitch rates when $\theta \approx 0$ are generally higher in the scheduled gain tests than in the single gain tests, see Figure 4.2. However, the rates were still not enough to be satisfactory for the pilot.

The first tuning $Q_\theta = 0$, $Q_{q_e} = 10$ was the most responsive according to the pilot out of all the tuning cases, including the scheduled gains. This was expected. The more aggressive controller tunings were all less responsive than desirable. However, the aircraft was percieved as more controllable in all closed-loop cases than in the open-loop test.

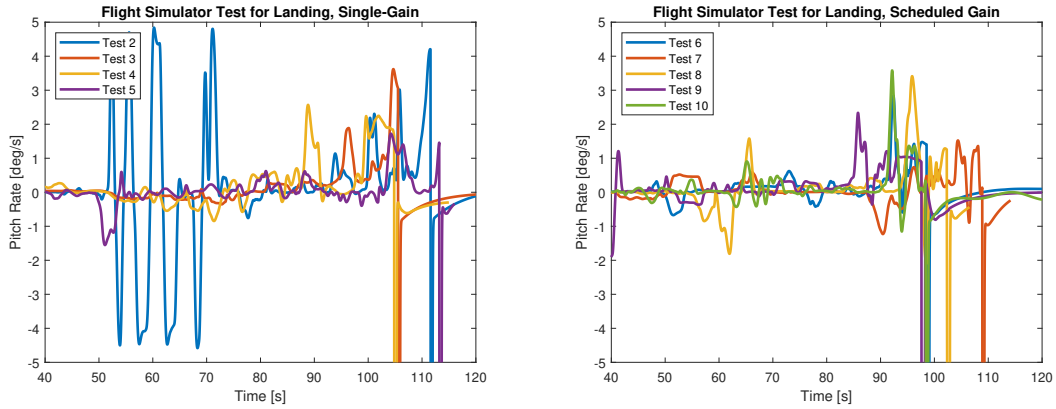

Figure 4.2: Pitch rate for landing with a) single-gain b) scheduled gain

In Figures 4.3 the velocities (measured as equivalent airspeed, EAS) is displayed for each test. The velocity has an important effect on the elevator authority, meaning that a higher velocity demands less elevator deflection to achieve the same pitch rate. For the single-gain controller the velocity is less important, since the controller will adapt the amount elevator deflection to any new gain in authority automatically.

The correct landing speed is within the 45-50 m/s range and this is achieved in all tests. From the figures it can be observed that the speed falls off fast when the pilot flares. This is true for both the single- and scheduled gain tests.

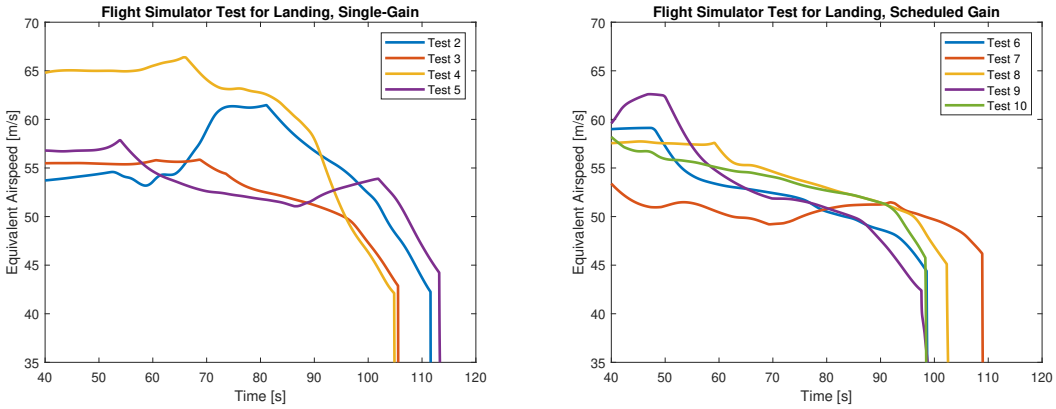

Figure 4.3: Equivalent airspeed for landing with a) single-gain b) scheduled gain

The velocity is important for the gain scheduling, since the equivalent airspeed is one of the scheduling parameters. For the scheduling to function as intended the aircraft should stay within the polytope. In Figure 4.4 the pitch attitude θ is plotted versus the equivalent airspeed EAS, along with the operating points used for computing the scheduled gains depicted as blue points. The nonexisting operating points for a pair of pitch attitude and equivalent airspeed values are depicted as red points (see Figure 3.18).

For all the tests using scheduled gain it can be observed that the aircraft exits the polytope during the flare when the equivalent airspeed goes below 45 m/s. When this occurs, the state feedback gain K freezes. The aircraft will thereafter operate with a K-matrix computed using a tuning scheduled for the last known pitch attitude within the polytope. For the tests 6-10, the aircraft will use the tuning scheduled for a pitch attitude of $\approx 7 - 9.5°$.

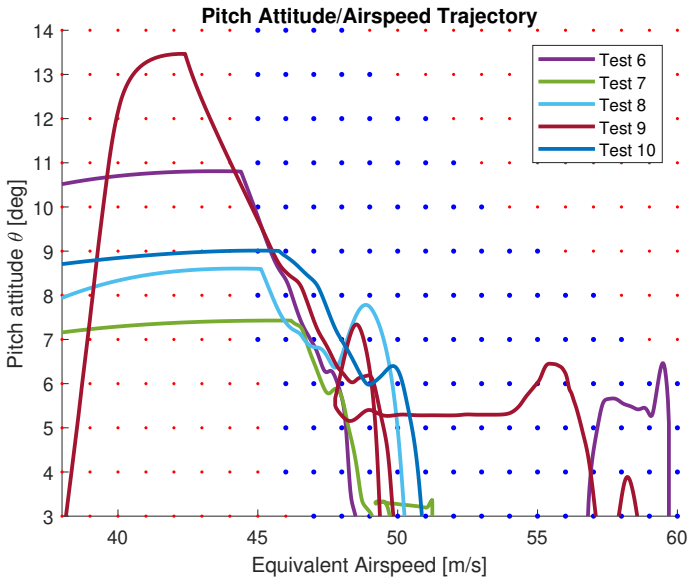

Figure 4.4: Pitch attitude θ plotted versus the equivalent airspeed EAS for flight test with scheduled gain

In Table 4.1 the results for the flight simulator landing tests are summarized. The maximal pitch rate, the maximal pitch, and a statement on whether a tailstrike has occurred or not is displayed for each test. The exact open-loop values were omitted, but the landing was in general hard to perform because of controllability issues and may not be completely accurate.

Landing Tests	Max Pitch Rate [deg/s]	Max Pitch at Touchdown [deg]	Tailstrike?
Test 2	5	15.8	Yes
Test 3	4	15	Yes
Test 4	2.5	17.8	Yes
Test 5	1.7	8.4	No
Test 6	3	13.4	No
Test 7	1.5	10.6	No
Test 8	3.3	8.4	No
Test 9	2.2	13.4	No
Test 10	3.6	9	No

Table 4.1: Results from the flight simulator tests

4.1.2 Takeoff

It is currently not possible to test the takeoff case in the flight simulator because of model deficiencies. The tests for the takeoff case is done in Simulink^{TM} and can be repeated in the flight simulator once the ground model is complete. However, these tests will lack valuable input from a pilot.

The results that will be presented in this section is done in two cases. Firstly when a pilot pitch up command is given once V_r is reached and secondly the command is given before V_r is reached. The pilot pitch up command is given as a step of maximum pitch for 10 seconds. It is important to note that a pilot wouldn't command the pitch in this way, but it is a good way to test the response when it can't be tested in the simulator. The tuning for the controller is presented in table 4.2

Test	**Level of Control**	Q_θ	Q_{q_e}
Test 1	Low	0	10
Test 2	Low	1	10
Test 3	Medium	3	8
Test 4	Tough	5	6
Test 5	Tough	6	4

Table 4.2: Single-gain tests for takeoff, re-stated from Table 3.17

Figure 4.5 and table 4.3 displays the results from when the speed $V_r = 93.6$ knots is reached. This is done by giving full pilot thrust command at timeinstance 30. Then at timeinstance 40 full pilot pitch command is given.

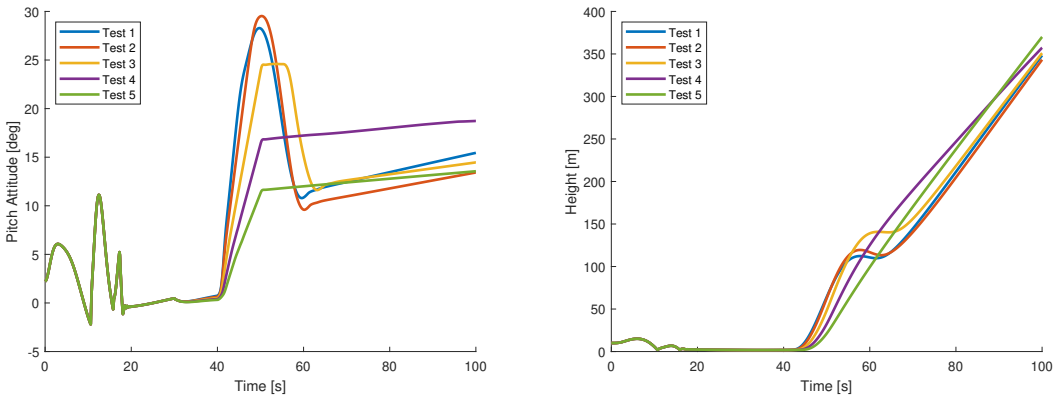

Figure 4.5: The response of the controller when V_r is reached, pitch angle to the left and height to the right.

It could be concluded that a tailstrike is avoided in all cases since the aircraft has gained enough height before the critical angle is reached. The results of these tests are presented in table 4.3

Takeoff Test	**Height above the ground when critical angle is reached [m]**	Tailstrike?
Test 1	4.47	No
Test 2	6.03	No
Test 3	11.78	No
Test 4	23.63	No
Test 5	Not reached	No

Table 4.3: Height above the gound when $\theta = 14.7$

Figure 4.6 and Table 4.4 displays the results when the speed V_r is not reached. This is done similarly to the previous simulation but with half the maximum pilot thrust command. It could be concluded that the aircraft is more prone to tailstrikes when the correct rotation speed is not yet reached. Which is reasonable since the aircraft will have a high enough speed to give the pilot pitch authority, but not high enough speed for the aircraft to leave the ground.

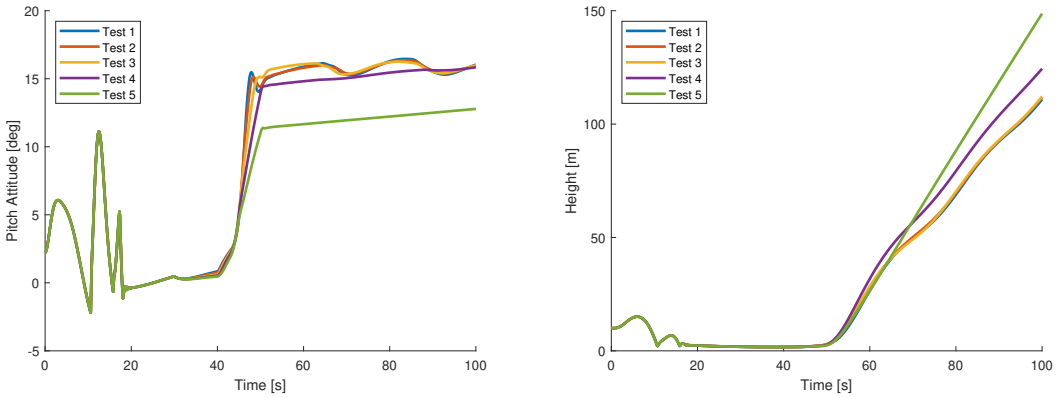

Figure 4.6: The response of the controller when V_r is not reached, pitch angle to the left and height to the right.

In this case a tailstrike is avoided in three out of five cases (see table 4.4). Meaning that a harsher tuning is needed for the single gain test if the correct speed V_r is not reached before the rotation is initialized.

Takeoff **Test**	**Height above the ground when critical angle is reached**	Tailstrike?
Test 1	2.16	Yes
Test 2	2.20	Yes
Test 3	2.343	Yes
Test 4	19.67	No
Test 5	Not reached	No

Table 4.4: Height above the gound when $\theta = 14.7$

To evaluate how well the controller preforms a similar test were done in open loop.

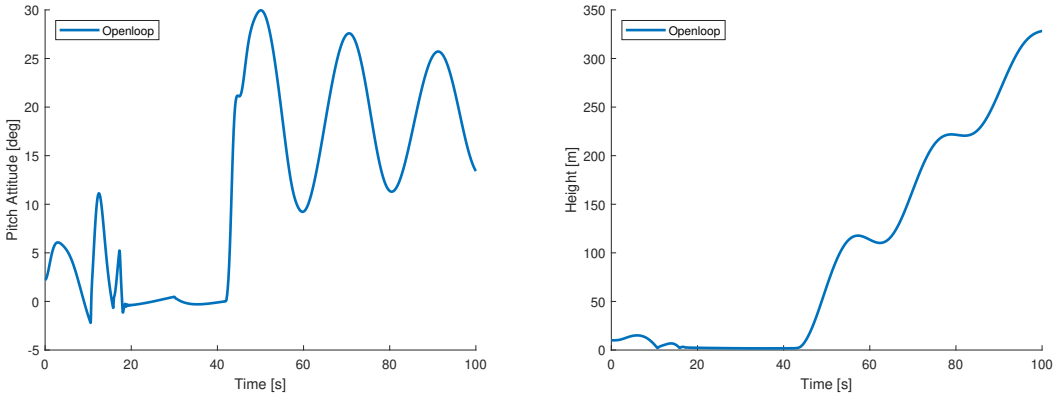

Figure 4.7: Open-loop response when V_r is reached, pitch angle to the left and height to the right.

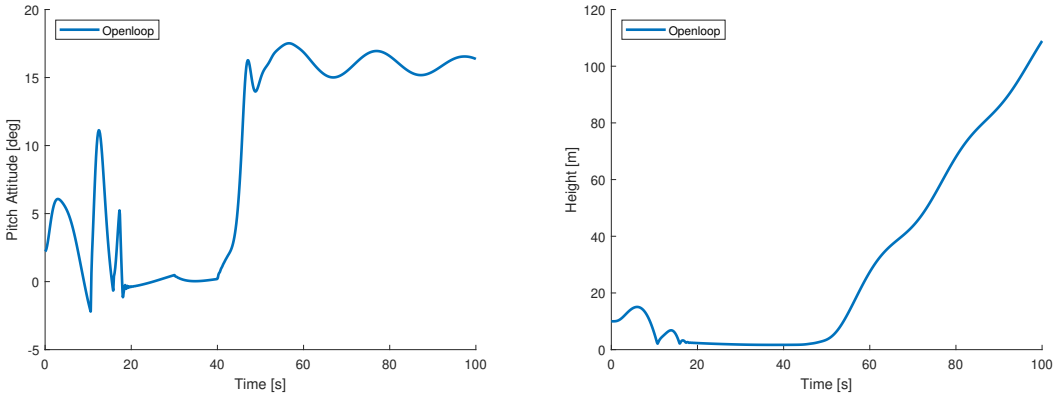

Figure 4.8: Open-loop response when V_r is not reached, pitch angle to the left and height to the right.

In the case where V_r is reached before the pilot pitch command is given the critical angle is reached when the aircraft is at an height of $H = 2.486$m resulting in a tailstrike. In this case even the controller with a soft tuning would prevent this from occuring. In the case where V_r is not reached before the pilot command is given there is a tailstrike at height of $H = 2.14$m, which also can be prevented by the controller although a tougher tuning for the controller would be needed.

5

Discussion

5.1 Modeling

Modeling of the aircraft has a direct impact on the performance of the controller, and as such it is valid to analyze the quality of it.

The takeoff case had multiple issues with the trimming of the aircraft that negatively affected the testing of the control design for this phase of flight. Since the aircraft model was not fit for standing on the ground, the aircraft had to be trimmed for flying conditions in the air and, because of this, a operating point with zero thrust and velocity could not be computed. Once at the simulation phase the thrust and velocity initial conditions had to be reduced to zero, altering the initial conditions produced by the trim. This would pose less of a problem if not the controller had been based on the linearization of the nonlinear model around the trim point. While the conceptual solution is still feasible, the state feedback matrix K is not entirely accurately computed for this state of the aircraft.

Also, altering the initial conditions of the trim caused the states to deviate from the *original* initial condition when fed back to the controller, which then the controller attempted to correct by feeding back extreme control signals. This was fixed by subtracting the original initial conditions from the states before entering the controller (instead of the updated versions), however in a real application they should be identical to the actual conditions. There are no signs of the conceptual solution being an invalid approach for preventing a tailstrike, however the model must first be allowed to trim correctly at ground level to do a correct flight testing and stability analysis of the controller.

5.2 Controller Design

In this section the controller design will be discussed, with a starting point in the results from the pilot tests. From there on the strengths and weaknesses of the two applications of the linear quadratic regulator will be discussed, alongside with some analysis and further recommendations.

5.2.1 Pilot Testing

This subsection will go over the results of the pilot testing, from the first few general observations to the specific results in the landing and takeoff tests, and finishing with some improvements that could be made to future flight testing.

General Observations

A general takeaway from the pilot testing was that the responsiveness of the aircraft was less for the closed-loop system than the open-loop system for a majority of the tuning cases (using both single- and scheduled gain). This is somewhat expected, since the premise of the controller is to reduce the authority of the pilot if the aircraft is at risk of a tailstrike, but this balancing of objectives is not trivial. However, the limitation may not purely rest in the tuning of the design parameters, but in the gains used to translate a pilot side stick command to a pitch rate reference. The gains currently used can generate a maximum pitch rate of 5 deg/second, and could be increased to enhance the responsiveness of the aircraft.

The second general takeaway from the closed-loop testing is that, while less responsive, the closed-loop system is considerably more controllable. This is a desirable feature. While poor responsiveness can be adjusted with different tunings and gains, adjusting hard-controllable and open-loop aircraft likely requires design changes to the aircraft. A closed-loop system comes with the ability of manipulating performance at a low cost.

Landing

In the landing tests a tailstrike was prevented in six out of nine tests, one using a single-gain controller with the toughest tuning and five (all) using the scheduled gain controller. There could be two explanations to these outcomes. The first explanation is that there is quota between the costs Q_θ and Q_{q_e} that can be regarded as critical to ensuring the prevention of a tailstrike. For example a tailstrike could still occur (using single-gain) with the costs $Q_\theta = 3$ and $Q_{q_e} = 8$, but not with the tuning $Q_\theta = 5$ and $Q_{q_e} = 6$. Approximately the same costs (as the latter combination) were applied in all of the scheduled gain tests once the attitude exceeded $7 - 8°$ of pitch attitude, suggesting that at this point the aircraft was so difficult to overrotate a tailstrike could not occur.

The second explanation is that with single-gain the pilot had become accustomed to the response rate and applies more force accordingly until the aircraft overrotates, but with the scheduled gain there is an element of surprise since the stronger controller action is reserved towards the end of the rotation.

Tailstrikes are (as earlier mentioned in the thesis) the most prevalent for landing operations, and although a considerable more amount of testing is required the controller evidently has the capability to prevent tailstrikes from occurring. The controller can both prevent drastic overrotations and slow down excessive flares, which are two prominent causes for tailstrikes. The controller has also shown to

introduce a good resistance to wind turbulence, which in the case of strong winds during landing should show itself powerful. Even if the tuning of the controller is a constant process (which can always be refined) the third cost schedule (Case 5: Medium) is according to our results sufficient to prevent a tailstrike while still keeping as much responsiveness as possible.

Takeoff

Altough there are alot of tailstrikes presented in the takeoff results it is quite unlikly that they will occur when a pilot is operating the aircraft. In the case where the correct speed is reached before the rotation is initiated, the controller manages to prevent a tailstrike with a low punishment eventough an excessive pilot pitch command is used. In the case where v_r is not it is important to note that this case is a combination of rotation at improper speed and an excessive pilot pitch command. The controller still manages to prevent a tailstrike from occuring with a tough tuning but struggles to do so with a low punishment. The disadvantage with using tough tuning is that the pilot will not be satsified with the response of the sidestick. To find a solution which has good tailstrike preventive characteristic and a good enough response more tests are needed to be done. Including a multiple gain scheduling and also pilot testing in the simulator.

Improvements to Flight Testing

To verify the controller design a pilot has been instructed to attempt to tailstrike during landing and takeoff operations. However, each test has only been applied once and with the same pilot. For future, more rigourous flight testing, multiple attempts should be recorded for each test case. This is to ensure that the results aren't one-time occurrences. Also, variations in timing and duration of the flare should be tested to better test the limits of the controller.

There are also standardized tests and scalings that are used for flight testing, like the Cooper-Harper scale, that should be applied. However, such tests required preparations that were left out because of time constraints.

5.2.2 Controller Solution and Single-Gain Feedback

In this subsection both the principal controller solution and the use of just a single state feedback matrix will be discussed. Even if based on the same principal solution, the analysis of the *scheduled* gain will be left for the next section.

The Benefits of Closed-Loop Control

The benefit of this closed-loop control over the open-loop approach is the ability to manipulate the controls and responses of the aircraft to ones liking. The gains, the settling times, and the response times can all be adjusted. They can also be adjusted such that they match the open-loop response to a degree, such that the transient from open-loop to closed-loop when the controller activates becomes unnoticeable.

This is not true in the moment, since the pilot noticed a considerable difference between open- and closed-loop control. This is largely due to an issue with the open-loop system however.

The closed-loop system can also be equipped with more functions. For now, the aircraft will keep the attained attitude without trimming. This was desirable for the pilot, but it is (in the moment) a deviation from the open-loop behaviour. This property can be removed by initiating a negative pitch rate reference signal such that the aircraft returns to the trimmed position. But, since this is closed-loop, the system response can be actively designed to be comfortable and intuitive to the pilot. Other functions can be included as well, and be implemented as a state machine.

General Stability and Robustness

The controller design in this thesis has relied on the existence of perfect sensor readings of all the states. This assumption will not hold in reality. The sensors will contain a bias in the readings, and to reconstruct states or filter the measurements an observer will most likely be needed. If the measurements continue to be biased this might need to be compensated for with a more conservative tuning to be on the safe side from exceeding θ_{strike}.

The incorporation of an observer or prevalence of measurement errors has the one significant downside in the loss of all robustness properties of the LQR. These robustness properties has allowed the single-gain controller to function for large deviations from the trim point and in the presence of wind turbulence. To allow for the same kind of performance levels one must begin to look for other, more robust controllers, such as the H_2 and H_∞ controllers.

The Impact of Trims

The trim has a large impact on the ability to tailstrike, and therefore multiple trims need to be tested. Different tunings might have to be used for different trims to ensure that the tailstrike preventive function is reliable.

Since the controller is computed using a linearized state space model around an operating point, the feedback gain will be proportional to the states' deviation from their operating point, $x - x_0$. The closer the operating point for the pitch attitude approaches $\theta_{strike} = 14.7°$ the less deviation $x - x_0$ is fed to the controller. If the pilot would trim at a higher attitude, the cost to that state θ must therefore be increased to compensate for the loss of margin to the critical attitude.

Soft vs Hard Limit

The controller design based on the linear quadratic regulator controller only applies soft limits on the pitch attitude, which suggests that a strong-willed pilot could still put the aircraft in the position for a tailstrike. The tailstrike can therefore not be prevented for all cases. For a absolute tailstrike prevention function hard limits

in controllers would need to be introduced. This could be done in multiple ways. One solution is to zero out the pitch rate reference q_{ref} when the pitch attitude approaches too close the critical attitude θ_{strike}, essentially freezing the attitude, or to implement an automatic pitch down command.

However, there are a number of disadvantages to hard limits. A hard limit would introduce (to the pilot) unappreciated nonlinearities in the stick command, potentially giving rise to a dead stick or unpredictable behaviour. As previously mentioned in section 1.5, the automatic pitch-down command has also been the cause of multiple aircraft accidents. A pilot prefers predictable and stable aircraft behaviour, and this is the benefit of a soft-limit controller. The second benefit of a soft-limit controller is the possibility to override it if another dire situation arises.

5.2.3 Scheduled Gain

It is clear however that a single-gain controller has the drawback of lacking the ability to combine the objective of responsiveness with that of tailstrike preventive properties. The main advantage of the multiple gain scheduling is that the cost to one ore more states can be set dynamically, balancing objectives at different ends of the polytope. The objective of high responsiveness can be fulfilled at low attitudes while the preventive properties are amplified at higher attitudes (dampening the responsiveness of the system), making gain scheduling a more desirable option than a single gain controller.

The Impact and Limitations of the Polytope

However, the usefulness of the gain scheduling is a function of the polytope. This was evident in the flight simulator landing tests (see section 4.1.1), where the aircraft exited the polytope by dropping to an equivalent airspeed below 45 m/s (Figure 4.4). Since there are no available gains computed for these specific flight conditions the last available one is used, whose tailstrike preventable properties are likely considerably lower if the aircraft exits the polytope at a attitude of $\theta < 10°$.

This has two implications. First, the tailstrike preventive properties of the controller is undermined and becomes unreliable. Being unreliable is a problem in itself, since the function's mere existence would induce a false sense of security for the pilot. The pilot could pitch-up and expect to become counteracted by the controller and hence overcompensates the stick command. If this counteraction is weaker than expected for a given attitude, the pilot could, in theory, overrotate.

Secondly, to avoid the controller from becoming unreliable the cost scheduled could use a conservative tuning, as in, applying a higher cost Q_θ at a lower attitude. With this approach the controller will be aggressively tuned for a larger portion of the polytope, suggesting that, even if the aircraft exits the polytope at a low attitude, it is likely that the controller is sufficient for preventing a tailstrike. This however defeats the second purpose with the scheduled gain, which was to keep a high responsiveness at lower attitudes.

The primary solution to this problem is to extend the polytope for more flight conditions. It should be extended for lower attitudes (including negative) and speeds, and certainly be extended for a combination of higher attitudes and speeds. One should first attempt to alter the trim settings by relaxing constraints or switching algorithm to produce more operating points for which a feedback gain K can be computed. It is likely however that the aircraft is outright not able to reach a steady-state at low speeds, regardless of trim settings. It should also be investigated if non-steady states could be used, just to add additional feedback gains for these dynamics.

The polytope should also be extended with more scheduling parameters, and begin to include the lateral dynamics such as the roll angle ϕ and sideslip angle β. If it, by relaxing constraints on the trim, would be possible to include the flight path angle γ or angle-of-attack α as a scheduling parameter in combination with the pitch attitude θ, it would be possible to investigate and incorporate stall prevention measures.

Stability of the Scheduled Gain

Another drawback with the scheduled gain is that the stability and robustness of the controller is difficult to guarantee. Recall that stability can only be concluded at the specific operating points at which the feeedbacks gains were computed. The gain scheduling approach needs extensive simulation testing to guarantee safety of the solution. Instability could be observed with numerous preliminary tunings of the gain schedule, and was usually expressed as oscillations before the control of the aircraft was lost. The causes can be multiple, such as too high controller gain for the most aggressive tunings, scheduling parameters changing at a higher rate than tolerable, or destructive transients.

The number of grid points could be increased to allow for more points at which the local stability is guaranteed, this can however come at the cost of computational complexity and eventual memory problems. The numerous linear parameter-varying tools in Matlab^{TM} could also be more extensively used to analyze and schedule gains over a more advanced polytope.

6

Conclusion and Further Work

In the end it could be concluded that there tends to be a higher risk of tailstrike during the landing phase compared to the take off. This is due to a multiple of reasons. In the takeoff case the pilot is suppose to start the rotaition when the speed V_r is reached. If this condition is fulfilled there is still a risk of tailstrike with a bad pilot if the aircraft is operated in openloop, even though that it is very unlikly. If the rotation is started before V_r is reached the likelihood of a tailstrike is increased, which motivates the use of a controller.

For the landing operation a gain scheduled linear quadratic regulator has shown good tailstrike preventive properties. Although not equipped with a hard limit, the controller counteracts the pilot enough at rising attitudes to lower the risks of tailstrike significantly. To make it fully reliable the polytope needs to be expanded such that there are ready and available gains even for less steady flight conditions. More stability and robustness analysis and a considerable amount of flight testing is needed to guarantee the safety of the gain scheduling. Also, introducing a specific schedule for pitch-down command to allow for better pilot handling qualities and lower pilot workload should be considered.

Bibliography

[1] Anderson, J. D. jr. (1989). *Introduction to flight* (3. ed.). McGraw-Hill.

[2] Anderson, J. D. (2011). *Fundamentals of aerodynamics* (5. ed. in SI units). McGraw-Hill.

[3] Asselin M.. (2021). *Operational Aircraft Performance and Flight Test Practices.* American Institute of Aeronautics and Astronautics (AIAA).

[4] Boeing Magazine (1998), *Tail Strike Avoidance.* Boeing Aeromagazine Archive, Issue 4, 1998. URL: https://www.boeing.com/commercial/aeromagazine/aero_04/tr/tr01/index.html

[5] Cashman, J.E., Kelly, B.D., Nield, B.N.. (2000) *What is Angle of Attack?, AERO*, Boeing Magazine Archives. Issue 12, 2000. URL: https://www.boeing.com/commercial/aeromagazine/aero_12/attack_whatisaoa.html

[6] Chilali, M., Gahinet, P., & Apkarian, P. (1997). *Robust pole placement in LMI regions.* Proceedings of the 36th IEEE Conference on Decision and Control, Decision and Control, 1997., Proceedings of the 36th IEEE Conference On, 2, 1291. https://doi.org/10.1109/CDC.1997.657634

[7] Chen, W.-K. (2005). *The electrical engineering handbook.* Elsevier.

[8] Chen, Y., Han, Z., and Gu, J.. (2019) *Analyzing the Causes of Tail Strike Event during Takeoff with Stepwise Regression*, 2019 1st IEEE International Conference on Civil Aviation Safety and Information Technology (ICCASIT), Kunming, China, 2019, pp. 418-424, doi: 10.1109/ICCASIT48058.2019.8973193.

[9] Committee On Transportation And Infrastructure (2020) *The Design, Development & Certification of the Boeing 737 Max.* URL: https://www.washingtonpost.com/context/final-house-committee-report-on-the-boeing-737-max/2ab7a376-79ec-4da4-bf0f-f7a4ecf8f4af/

[10] Dewitt, W.M., Evans, M.R., Wells, S.L. (2007). *Aircraft tailstrike avoidance system.* (EN. Patent No. EP1727012) European Patent Office. URL: https://register.epo.org/application?number=EP06076438

[11] Doyle, J. (1978). *Guaranteed margins for LQG regulators*. IEEE Transactions on Automatic Control, Automatic Control, IEEE Transactions on, IEEE Trans. Automat. Contr, 23(4), 756–757. https://doi.org/10.1109/TAC.1978.1101812

[12] European Commission, *Reducing emissions from aviation*, URL: https://climate.ec.europa.eu/eu-action/transport-emissions/reducing-emissions-aviation

[13] Federal Aviation Administration (2016). *Pilot's Handbook of Aeronautical Knowledge*. U.S Department of Transportation.

[14] Glad, T., & Ljung, L. (2000). *Control theory.: multivariable and nonlinear methods*. Taylor & Francis.

[15] Gudmundsson, S. (2022). *General Aviation Aircraft Design: Applied Methods and Procedures*. 2nd Edition. Elsevier Science & Technology.

[16] Hardiman, J., (2022 Nov. 26th), *Wreckage Still Being Discovered: The Story Of Japan Airlines Flight 123*, Simple Flying. URL: https://simpleflying.com/japan-airlines-flight-123-story/

[17] Hjartarson, A., Seiler, P., Packard, A. (2015) *LPVTools: A Toolbox for Modeling, Analysis, and Synthesis of Parameter Varying Control Systems*. IFAC-PapersOnLine, Volume 48, Issue 26, 2015, Pages 139-145, ISSN 2405-8963, https://doi.org/10.1016/j.ifacol.2015.11.127.

[18] Howard, C., & Joseph C., B. (1973). *A Stall/Spin Prevention Device for General-Aviation Aircraft*. SAE International. https://doi.org/10.4271/730333

[19] Huynh, V.N.. (2019) *Tailstrike Awareness System*. (European Patent Publication No. EP3530562) European Patent Office. URL: https://register.epo.org/application?number=EP19158293

[20] Ishihara, Y., Johnson, S.. (2012) *Systems and methods for alerting potential tailstrike during landing*. (European Patent Publication No. EP2444322) European Patent Office. URL: https://register.epo.org/application?number=EP11184757

[21] Kermode, A.C., Barnard, R.H., Philpott, D.R.. *Mechanics of Flight* (2006) 11th Edition. Pearson Education Limited.

[22] Larsson, R. (2019). *Flight Test System Identification* (PhD dissertation, Linköping University Electronic Press). https://doi.org/10.3384/diss.diva-156694

[23] Mathworks (2023). *Dryden Wind turbulance*. URL: https://se.mathworks.com/help/aeroblks/drydenwindturbulencemodelcontinuous.html

[24] Mathworks (2023). *lqr*.

URL:https://se.mathworks.com/help/control/ref/lti.lqr.html

[25] Mathworks (2023). *What is Model Predictive Control?*. URL: https://se.mathworks.com/help/mpc/gs/what-is-mpc.html

[26] Mathworks (2023). *findopOptions*.
URL: https://se.mathworks.com/help/slcontrol/ug/findopoptions.html

[27] Montalvo, C., Costello, M.. (2015). *Meta Aircraft Flight Dynamics*. Journal of Aircraft, 52, 107-115.

[28] Mix, D. R., Koenig, J. S., Linda, K. M., Cifdaloz, O., Wells, V. L., & Rodriguez, A. A. (2004). *Towards gain-scheduled H/sup /spl infin// control design for a tilt-wing aircraft*. 2004 43rd IEEE Conference on Decision and Control (CDC) (IEEE Cat. No.04CH37601), Decision and Control, 2004. CDC. 43rd IEEE Conference on, Decision and Control, 2, 1222. https://doi.org/10.1109/CDC.2004.1430208

[29] Palomeque, M.. (2008) *A320/ Prevention of tailstrikes*. Safety First Magazine, Airbus. URL: https://safetyfirst.airbus.com/a320-prevention-of-tailstrikes/

[30] Sachdeva, N., *Achieving greener flight: Navigating the roadmap to True Zero emissions*. Roland Berger consulting. URL: https://www.rolandberger.com/en/Insights/Global-Topics/Sustainable-Aerospace-and-Aviation.html

[31] Stevens, B. L., Lewis, F. L., & Johnson, E. N. (2015). *Aircraft Control and Simulation: Dynamics, Controls Design, and Autonomous Systems* (3rd ed.). John Wiley & Sons, Incorporated.

[32] Stinton, D. (1998), *The Anatomy of the Airplane*, 2nd Edition. Wiley-Blackwell.

[33] United States Department of Defense (1990) *Flying Qualities of Piloted Aircraft*, Volume MIL-F-1797A.

[34] Van Kampen, Erik-Jan & Chu, Q.P. & Mulder, J.A.. (2007). *New Approach for Nonlinear Aircraft Trim using Interval Analysis.* 4. American Institute of Aeronautics and Astronatics. 10.2514/6.2007-6766.

[35] Visioli, A. (2006). *Practical PID Control*. [electronic resource] (1st ed. 2006.). Springer London.

[36] Weinmann, A. (1991). *Uncertain Models and Robust Control*. [electronic resource] (1st ed. 1991.). Springer Vienna.

[37] Wong, D., (2022, May 22th). *Deadly Metal Fatigue: The Story Of China Airlines Flight 611*, Simple Flying.
URL: https://simpleflying.com/china-airlines-flight-611-metal-fatigue-story/

[38] Yechout, T. R., & Staff, A. I. of A. and A. (2003). *Introduction to Aircraft Flight Mechanics*. American Institute of Aeronautics and Astronautics.

DEPARTMENT OF SOME SUBJECT OR TECHNOLOGY
CHALMERS UNIVERSITY OF TECHNOLOGY
Gothenburg, Sweden
www.chalmers.se

CHALMERS
UNIVERSITY OF TECHNOLOGY